

See discussions, stats, and author profiles for this publication at: <https://www.researchgate.net/publication/51719137>

The structure-antituberculosis activity relationships study in a series of 5-aryl-2-thio-1,3,4-oxadiazole derivatives

ARTICLE *in* BIOORGANIC & MEDICINAL CHEMISTRY · NOVEMBER 2011

Impact Factor: 2.79 · DOI: 10.1016/j.bmc.2011.09.038 · Source: PubMed

CITATIONS

9

READS

53

9 AUTHORS, INCLUDING:



Fliur Macaev

Academy of Sciences of Moldova, Institute ...

43 PUBLICATIONS 388 CITATIONS

SEE PROFILE



Veaceslav Boldescu

Academy of Sciences of Moldova

14 PUBLICATIONS 28 CITATIONS

SEE PROFILE



Athina A Geronikaki

Aristotle University of Thessaloniki

94 PUBLICATIONS 1,672 CITATIONS

SEE PROFILE



Robert C Reynolds

University of Alabama at Birmingham

130 PUBLICATIONS 3,017 CITATIONS

SEE PROFILE



The structure–antituberculosis activity relationships study in a series of 5-aryl-2-thio-1,3,4-oxadiazole derivatives

Fliur Macaev^{a,*}, Zinaida Ribkovskaia^a, Serghei Pogrebnoi^a, Veaceslav Boldescu^a, Ghenadie Rusu^a, Nathaly Shvets^b, Anatholy Dimoglo^{b,*}, Athina Geronikaki^c, Robert Reynolds^d

^a Institute of Chemistry, Academy of Sciences of Moldova, Academiei Str. 3, Chisinau MD2028, Republic of Moldova

^b Gebze Institute of Technology, PK-141, Gebze/Kocaeli 41400, Turkey

^c Aristotelian University of Thessaloniki, Thessaloniki 54124, Greece

^d Southern Research Institute, Birmingham, AL 35255-5305, USA

ARTICLE INFO

Article history:

Received 13 June 2011

Revised 11 September 2011

Accepted 21 September 2011

Available online 29 September 2011

Keywords:

Antituberculosis activity

Structure–activity relationships

Electronic-topological method

Neural networks

Docking

ABSTRACT

A series of 82 5-aryl-2-thio-1,3,4-oxadiazole derivatives were screened for their anti-mycobacterial activities against *Mycobacterium tuberculosis* H37Rv. The synthesized compounds **30–37** appeared to be the most active derivatives exhibiting more than 90% inhibition of mycobacterial growth at 12.5 µg/mL. Structure–activity relationships study was performed for the given series by using the electronic-topological method combined with neural networks (ETM–NN). A system for the anti-mycobacterial activity prediction was developed as the result of training associative neural network (ASNN) with weights calculated from projections of a compound and each pharmacophoric fragment found on the elements of the Kohonen's self-organizing maps (SOMs). From the detailed analysis of all compounds under study, the necessary requirements for a compound to possess antituberculosis activity have been formulated. The analysis has shown that any requirement's violation for a molecule implies a considerable decrease or even complete loss of its activity. Molecular docking studies of the compounds allowed shedding light on the binding mode of these novel anti-mycobacterial inhibitors.

© 2011 Elsevier Ltd. All rights reserved.

1. Introduction

Tuberculosis (TB) remains the number one killer infectious disease affecting adults in developing countries. TB is a global emergency and is amongst the worldwide health threats today.¹ The situation is more complicated when one considers countries such as India where TB disproportionately affects the young. India accounts for one-third of the global TB burden, with 1.8 million developing the disease each year and nearly 0.4 million dying due to TB annually.

The World Health Organization (WHO) estimates that the largest number of new TB cases in 2004 occurred in WHO's South-East Asia Region, which accounted for 33% of incident cases globally. However, the estimated incidence per capita in sub-Saharan Africa is nearly twice that of the South-East Asia Region, at nearly 400 cases per 100,000 population.^{2,3}

Until 50 years ago, there were no medicines to cure TB. Now, strains that are resistant to single drugs have been documented in every country surveyed, and unfortunately, strains of TB resistant to all major anti-TB drugs have emerged. Drug-resistant TB is

caused by many factors: inconsistent or partial treatment and lack of compliancy (sometimes patients do not take all their medicines regularly for the required period because they start to feel better), prescription of wrong treatment regimens, or unreliable drug supply. A particularly dangerous form of TB is that caused by multi-drug-resistant TB (MDR-TB), defined as bacilli resistant to at least isoniazid and rifampicin, the two most powerful anti-TB drugs.^{4,5} While drug-resistant TB is generally treatable, it requires extensive chemotherapy (up to 2 years of treatment) that is often prohibitively expensive (often more than 100 times more expensive than treatment of drug-susceptible TB), in addition to being more toxic to patients. Noteworthy, the development of drug resistance also involves other poverty-related diseases, such as malaria and HIV/AIDS.^{4–8}

Over the last two decades current control efforts are severely hampered due to *Mycobacterium tuberculosis* is a leading opportunistic infection in patients with the acquired immune deficiency syndrome and also due to the spread of multidrug-resistant strains (MDR-MTB). Problems in the chemotherapy of tuberculosis arise when patients develop bacterial resistance to the first-line drugs: isoniazid (INH), rifampicin (RIF), etambutol (ETH), streptomycin (STR), and pyrazinamide (PYR). The emergence of new strains of *M. tuberculosis* resistant to some or all current antituberculosis drugs is a serious and crescent problem.⁹

* Corresponding authors. Tel.: +90 262 605 32 06; fax: +90 262 653 84 90 (A.D.).
E-mail addresses: flimacaev@cc.acad.md (F. Macaev), dimoglo@gyte.edu.tr (A. Dimoglo).

The current second-line drugs used in lengthy combination therapies to treat MDR-TB (typically over 2 years) mostly have reduced potency and (or) greater toxicity than existing first-line agents, and they may be largely ineffective against extensively drug-resistant tuberculosis (XDR-TB).¹⁰

Since no effective vaccine is available, the major strategy to combat the spreading of TB is the chemotherapy.¹¹ The ever-increasing resistance, toxicity and side effects of currently used antituberculosis drugs, together with the absence of their bactericidal activity, highlight the need for new, safer and more effective antituberculosis drugs.

1,3,4-Oxadiazoles form an important class of five-member heterocyclic compounds with a wide range of biological activities.¹¹ The importance of the oxadiazoles' nucleus is well established in agricultural and pharmaceutical chemistry as far as its corresponding derivatives are used as antipyretic, analgesic, antidepressant, antimicrobial,¹² antiviral, fungicidal, antineoplastic,¹¹ anti-inflammatory agents, central nervous system stimulants, and anticonvulsive, anticancer, and antihypertensive agents.¹³ Their important structural characteristic is the presence of two aromatic rings spaced by a heteroatom.¹³

The knowledge of quantitative relationships between chemical structure and biological activity is an essential prerequisite for the effective search for biologically active compounds.¹⁴ Earlier it was reported that a number of 2,5-disubstituted-1,3,4-oxadiazoles have been designed, synthesized, and screened for their antituberculosis activity against *M. tuberculosis* H37Rv.¹⁵ The compounds obtained have been tested according to the model developed in this study.

Anti-bacterial and -tuberculosis activities of compounds possessing azole ring have been reported in numerous studies.^{16–19} As a part of our ongoing studies in developing of new active compounds with anti-mycobacterial activity we report here a multi-step synthesis of 5-aryl-2-thio-1,3,4-oxadiazoles and our efforts to relate biological activity data to the nature of substituents in these compounds. Better understanding of structural requirements to substituted-1,3,4-oxadiazole derivatives that cause the antituberculosis activity of the latter, will help us to identify lead compounds for our future work.

A combined approach that is known as electron-topological method (ETM), followed by the artificial neural networks application to its results (in short, ETM-ANNs approach²⁰) was used in order to find more potent and selective antimicrobial agents against *M. tuberculosis* H37Rv. Both ETM and ETM-ANNs approaches have already been successfully applied to a wide enough variety of tasks related to the structure–activity relationships (SAR) investigations.^{21–26}

2. Syntheses and bioactivity estimation

The synthesis of target 1,3,4-oxadiazoles was accomplished by the following synthetic route (Fig. 1). Due to the presence of two high reactive groups in molecules **1**, **2**,²⁷ the –SH group alkylation reaction and addition of different nucleophiles to isothiocyanate group can lead to a large number of new compounds.

At the outset of this study it was observed that reactions of 2-mercapto-5-(4-isothiocyanatophenyl)-1,3,4-oxadiazole **1** with different amines in refluxing benzene gave corresponding substituted thioureas **3–11** with 68% up to 92% yield. Sulfides **12–19** can be prepared by the treatment of thiol **1** with alkyl halides. Depending on the nature of the alkylating reagent, the synthesis was carried out either in acetone in the presence of Et₃N (compounds **12–14**, **16–19**), or in DMF in the presence of K₂CO₃ (compound **15**). In case of compound **13**, the screening of the ratio of

substrate to reagent revealed that 1.0 equiv of **1** and 1.0 equiv of 4-(chloromethyl)pyridine hydrochloride to 2.0 equiv. of Et₃N was the optimal ratio. Further, reactions of 2-S-substituted-5-[(4)-isothiocyanatophenyl]-1,3,4-oxadiazoles **12–19** with amines have led to thioureas **20–38** with high yields.

During this investigation, a variety of amines were tested afterwards in the selected reaction of substrate **2** in boiling benzene (compounds **39–47**). As shown, hydrazine gives the best result (84% yields) among the tested models (Table 2, entry **44**). The optimized protocol was then expanded to a variety of BrCH₂-activated alkylating reagents and 2-mercapto-5-(3-isothiocyanatophenyl)-1,3,4-oxadiazole **2**. Variations of electronic properties of the substituents were tolerable, with yields ranging from 70% to 88% (entries **48–55**).

More important is that under the optimal conditions, two-component reactions between isothiocyanates **48–52**, **54**, **55** and amines proceeded smoothly and provided the desired products in good to excellent yields. It is worth noting that the reaction between **54** and 25% aq ammonia proceeded cleanly for only 3 h and afforded the corresponding 1,3,4-oxadiazole **68** in 87% yield (entry **68**). Synthesized compounds were characterized both by elemental and spectroscopic analyses (IR, NMR). Table 1 contains data on the structures of all compounds in this series.

The synthesized compounds were tested for their in vitro anti-mycobacterial activities against *M. tuberculosis* H37Rv on the BACTEC 12B medium using a broth microdilution assay, the Microplate Alamar Blue Assay (MABA).²⁸ Rifampicin was used as a standard in the anti-mycobacterial assays. The results of antitubercular activity are reported in Table 1.

The initial isothiocyanates (**1**, **2**) showed low inhibitory activity (2% and 9%, respectively). Compounds (**12–19**) derived from isothiocyanate **1** exhibit moderate activity (12–56%), except of compound **18** (2%), while compounds (**48–55**) derived from isothiocyanate **2** are completely inactive. The best antitubercular activity was observed for compound **19** (56%) followed by compound **12** (37%). It seems that bulky substituents in position 2 of the benzene ring are not favorable for the antitubercular activity.

It should be mentioned that compounds **4**, **23–25**, **27–37**, and **75** (58–98%) were the most active among the compounds tested. A significant increase of activities (up to 90%, 96%, and 98%) can be observed in the series of derivatives with monoethanolamine residues, substituted to the mercapto-group with 4-fluorophenacyl, phenacyl, allyl, and 2,4-dichlorophenacyl, respectively (compounds **29**, **32**, **33**, and **36**).

All investigated monosubstituted thioureas, derivatives of 4-aminobenzoic acid have been substituted on the SH-group, show high percents of inhibition. Thus, for example, derivatives of this type with residues of pyrimidine, benzyl, allyl and γ -picolyl (compounds **28**, **30**, **35**, and **37**) showed the activity indices as 87%, 91%, 98%, and 97% of inhibition, respectively. Also, very high indices of activity are observed for phenacylated derivatives in this series; as an example, compounds **27** and **31** with residues of phenacyl and 2,4-dichlorophenacyl have indices of activity equal to 61% and 93%, correspondingly.

In the investigated group of 1,3,4-oxadiazoles, derivatives of 4-aminobenzoic acid show a greater activity than corresponding *meta*-isomers, in most cases. Also, it is important to mention that the best activity indices are shown by 1,3,4-oxadiazoles on the basis of ammonia and monoethanolamine substituted on the mercapto-group. Among them, the best result of 98% was exhibited by compound **35** (monosubstituted thiourea) with an allylated fragment of the thiolic group and also by compound **36** being 2,4-dichlorophenacylated derivative with a monoethanolamine residue.

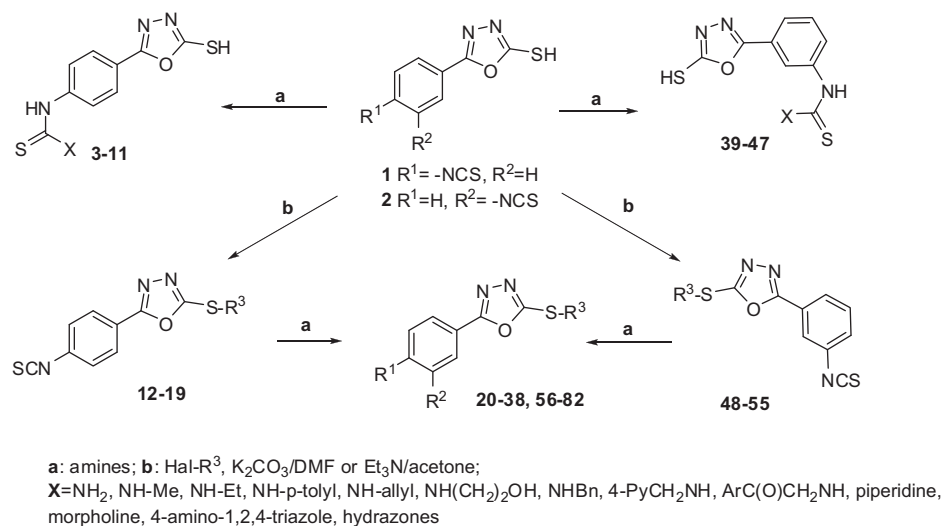


Figure 1. Synthesis of 5-aryl-2-thio-1,3,4-oxadiazole derivatives.

3. Computational methods

3.1. Docking studies

Docking as one of approaches to computer-assisted molecular modeling (CAMM) plays an essential role in the design of potential ligands that are both sterically and chemically compatible with the binding site of a target bio-macromolecule.^{29,30} When performed with default settings, docking reveals a number of possible conformations and orientations for the inhibitors at the binding site. Knowing the binding site conformations helps to show the important interactions that stabilize the complex ligand–receptor.

Initial molecular structures for docking were found from the package of quantum-chemistry programs ‘gaussian03’. All structures were optimized in the aqueous surroundings for further use.

As far as the structures in view are rigid molecular skeletons of the heterocyclic and ring form, and flexibility of their bonds is restricted, the usage of different optimizing methods causes very similar results. Structure optimization with docking is useful when compounds are flexible enough and have a lot of conformations. Docking could help to select an appropriate conformer in this case.

Crystal structure of the conserved hypothetical protein Rv1155 from *M. tuberculosis* was obtained from the Protein Data Bank (<http://www.rcsb.org>) under the Accession Code 1CI0.pdb (unpublished data).^{31–33} Pyridoxamine 5'-phosphate oxidase (PNPOx) is the smallest member of the flavin-containing oxidase family that catalyses the oxidation of pyridoxamine-5-P (PMP) and pyridoxine-5-P (PNP) to pyridoxal-5-P (PLP). This reaction serves as the terminal step in the de novo biosynthesis of PLP in *Escherichia coli* and as a part of the salvage pathway of this coenzyme in both *E. coli* and mammalian cells. A 10 Å sphere around the center of the binding pocket was defined as binding pocket for the docking.

Molecular mechanics techniques were used to minimize the ligand energy in the binding pocket, starting from a series of random positions and orientations within the binding site. The ligand structures had been energy-minimized by using the MMFF94s force field and the conjugated gradient method, until the default derivative convergence criterion of 0.05 kcal/(mol Å) was reached.

For the docking studies we used Molecular Operating Environment (MOE) software running on Windows-based PC³⁴ to estimate free energy of binding of the ligand in the poses given. The docked poses were scored using a London dG scoring function for finding the best docking pose. The protein–ligand complexes of protein

Rv1155 from *M. tuberculosis* were minimized up to a gradient of 0.01 kcal/(mol Å), and hydrogens were added using the force field AMBER99. Charges on the protein were assigned using the force field AMBER99, while the charges on the ligands were assigned by using force field MMF94X. The final energy was calculated using the Generalized Born solvation model (GB/VI).

3.2. ETM method

To begin with, each molecular structure is represented as a matrix called electron-topological matrix of conjunction (ETMC), which includes values of basic properties related to atoms and bonds of a molecule (charges, HOMO/LUMO orbitals, atomic distances, etc.).

In accordance with the main steps of the ETM-study, optimized geometry data and electronic characteristics calculated from the semi-empirical AM1 method^{35,36} are used in ETMCs that have been formed previously for all compounds (82 molecules). By this, effective charges on atoms (q_i , local atomic characteristics) were chosen as diagonal elements for the matrices; and either values of a bond characteristic (here, Wiberg's indices, W_{ij} , for bonds) or optimized distances (R_{ij} , in Å), otherwise, were used as their off-diagonal elements.

All compounds fall into classes of *active* molecules (17 mol, inh % >55), *low active* molecules (17 mol, 16 < inh % <55) and *inactive* ones (48, mol, inh % <15), in a natural way. Optimal values of allowable variations that have been found in the process of the matrices comparison (when testing if their atoms and bonds match) were found as $\Delta_1 = \pm 0.07$ for diagonal elements (q_i) and $\Delta_2 = \pm 0.20$ for off-diagonal values (W_{ij} and R_{ij}). To determine the most informative activity features, the lowest level of probabilistic estimations, P_a , was taken as 0.80.

$$P_a = (n_1 + 1)/(n_1 + n_2 + 2).$$

Here n_1 is the number of molecules possessing the \mathbf{S}_i activity fragment (pharmacophore) in the class of active compounds, and n_2 has the same meaning but in the class of inactive compounds (anti-pharmacophore), as found by the ETM.

To have more stable activity fragments, *every* active compound was used as a *template* for comparison with the rest of ETMCs in the course of the ETM study. After all ETMCs (i.e., active and inactive ones) had been processed, two corresponding sets of their common fragments (i.e., pharmacophores and anti-

Table 1 (continued)

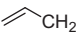
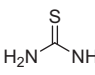
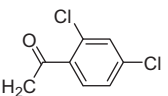
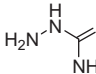
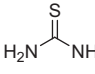
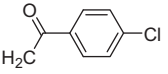
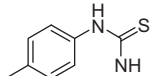
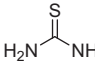
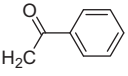
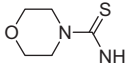
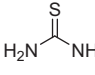
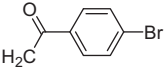
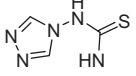
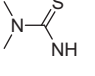
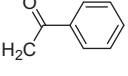
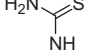
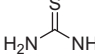
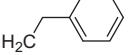
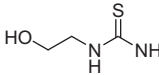
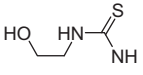
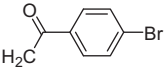
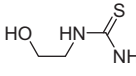
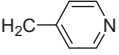
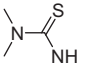
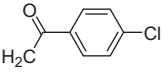
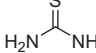
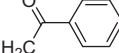
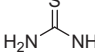
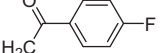
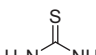
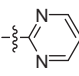
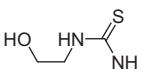
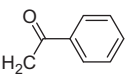
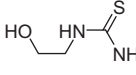
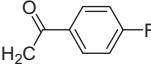
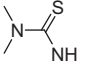
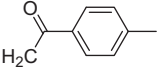
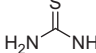
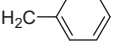
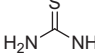
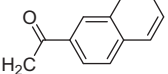
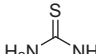
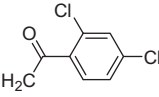
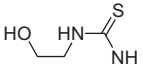
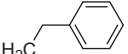
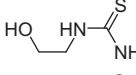
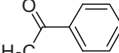
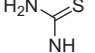
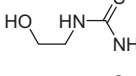
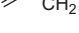
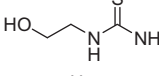
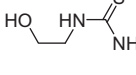
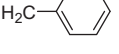
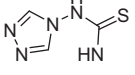
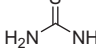

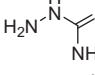
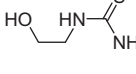
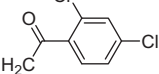
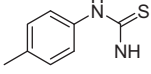
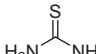
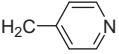
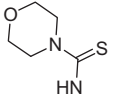
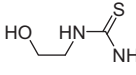
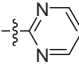
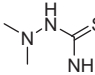
No.	R ¹	R ²	R ³	Inh (%)	No.	R ¹	R ²	R ³	Inh (%)
19	SCN	H		56	60	H			0
20		H	Me	0	61	H			0
21		H	Me	17	62	H			0
22		H	Me	0	63	H			6
23		H	Me	58	64	H			9
24		H	Me	78	65	H			16
25		H	Me	67	66	H			17
26		H		25	67	H			18
27		H		61	68	H			19
28		H		87	69	H			12
29		H		90	70	H			10
30		H		91	71	H			16
31		H		93	72	H			13
32		H		96	73	H		Me	25
33		H		96	74	H		Me	8
34		H		97	75	H		Me	58
35		H		98	76	H		Me	0
36		H		98	77	H		Me	21
37		H		97	78	H		Me	0
38		H		14	79	H		Me	8

Table 1 (continued)

No.	R ¹	R ²	R ³	Inh (%)	No.	R ¹	R ²	R ³	Inh (%)
39	H		H	0	80	H			1
40	H		H	16	81	H			0
41	H		H	20	82	H			0

pharmacophores) were obtained. These sets are already capable to assist experts in computer screening of new drug prototypes as well as in forecasting their activities.

3.3. ETM-ANNs approach

As seen, the aim of the ETM approach is to find molecular fragments (pharmacophores) common for the structures of all active compounds (for an activity selected) and absent in all inactive compounds with similar structures. The set of pharmacophores and antipharacophores revealed as the result of the ETMCs analysis, are basic molecular substructures that form a system for the given activity prognostication. The system can be used for testing newly synthesized compounds, so as for the computer modeling of new candidates for the purposeful syntheses.^{37–40}

However, the procedure of the activity prediction is difficult enough and needs the expert's participation. To automate this procedure, the ETM application was followed by the ANNs application (with unsupervised and supervised learning algorithms), and, as a result, these calculations were named as the ETM-ANNs combined approach.²⁰ The ANNs application uses data resulting from the ETM calculations (corresponding electron-topological submatrices of contiguity for pharmacophores and anti-pharmacophores, ETSC, in short) as input for a new algorithm developed on the base of Volume Learning Algorithm that had been created previously for the analysis of CoMFA data.^{41,42} This algorithm is implemented as a recurrent iterative application of the Kohonen self-organizing maps (SOMs) and associative neural networks (ASNNs).^{43,44} The general block-schema of the ETM-ANNs data analysis is shown in Figure 2.

According to this algorithm, its main steps are as follows:

- (1) Form the initial set of input data (ETM-data, such as ETMCs, pharmacophores and anti-pharmacophores).

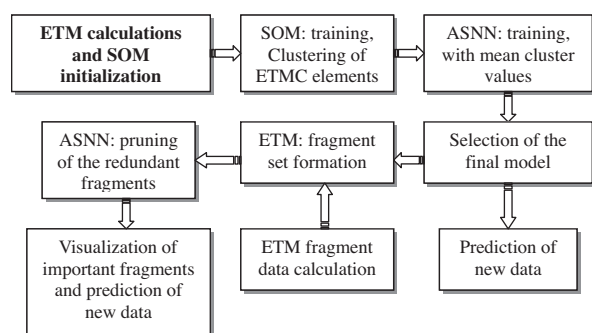


Figure 2. Block-schema of data analysis by means of ETM-ANN approach.

- (2) Initialize the Kohonen's network parameters; and, for each molecule, calculate clusters from its ETMC. The initial size of Kohonen's maps is taken as $S = 2 * S_{ETMC}$, where S_{ETMC} is the size of the largest molecular matrix.
- (3) Find common ETMCs fragments. For each fragment, calculate its projection on the units of the Kohonen's SOM. Calculate the *projection error* (E_q). Calculate the *weight* of each fragment ($1/E_q$) and create new data set by using the calculated fragment weights as parameters.
- (4) Analyze ETM-data as to fragments (i.e., ETSC) by using ASNNs; calculate the *average prediction error* (E_c).
- (5) Compare the E_c value to that one found at the preceding stage of learning, E_p (initially, $E_p = 10e-3$). If $E_c < E_p$, the current projection of the ETSC for the fragment is saved.
- (6) Decrease the size of the Kohonen's map.
- (7) Repeat steps 2–6 until the map size, S , decreases to S_{min} (S_{min} equals to eight nodes).
- (8) Select the best ETMC fragments' projections, relative to the minimal value of E_c , and predict the activity of new compounds.
- (9) Select the most informative ETMC fragments (after the ASNN training) by using special *pruning methods*.^{45,46}
- (10) Predict activities of new compounds.

The optimized ETMC fragments were used to visualize those regions of molecules under study that were found to be important for the analyzed activity demonstration by the molecules.

4. Results and discussions

4.1. Docking analysis

Docking of active compound **33** in Rv1155 shows that this compound docks well in the active site that consists of such amino acids as Ser144, Arg140, Lys78, Tyr88, Ile74, Leu75, and Leu76 (Fig. 3a). The oxygen of the hydroxyl group forms hydrogen bonds with Ser 144 (distance 2.70 Å) and Arg140 (distance 2.64 Å) of the protein. The oxadiazole ring is located in the vicinity of amino acids Leu76 and Leu75. The nitrogen of oxadiazole forms a hydrogen bond with Leu76 (distance 2.65 Å). Four of amino acids show a sidechain and backbone *acceptor* properties. Three of amino acids (Leu75, Leu76, and Ile74) show backbone *donor* properties. The phenyl ring settles in a hydrophobic cavity lined by Lys78, Tyr88, and Ser89. The dichlorophenyl ring (compounds **31** and **36**) is optimally oriented to make aryl cation interaction with the Arg140 (see Fig. 3b). According to docking results, compounds **31** and **36** exhibit a binding mode similar to that of compound **33**.

It is interesting to note that inactive compounds **60** and **20** (Fig. 3c and d) with different structures have close values of weak binding affinity. As seen from the docking studies, compound **60** in Rv1155 docks well in the active site that consists of the amino acids Ser89,

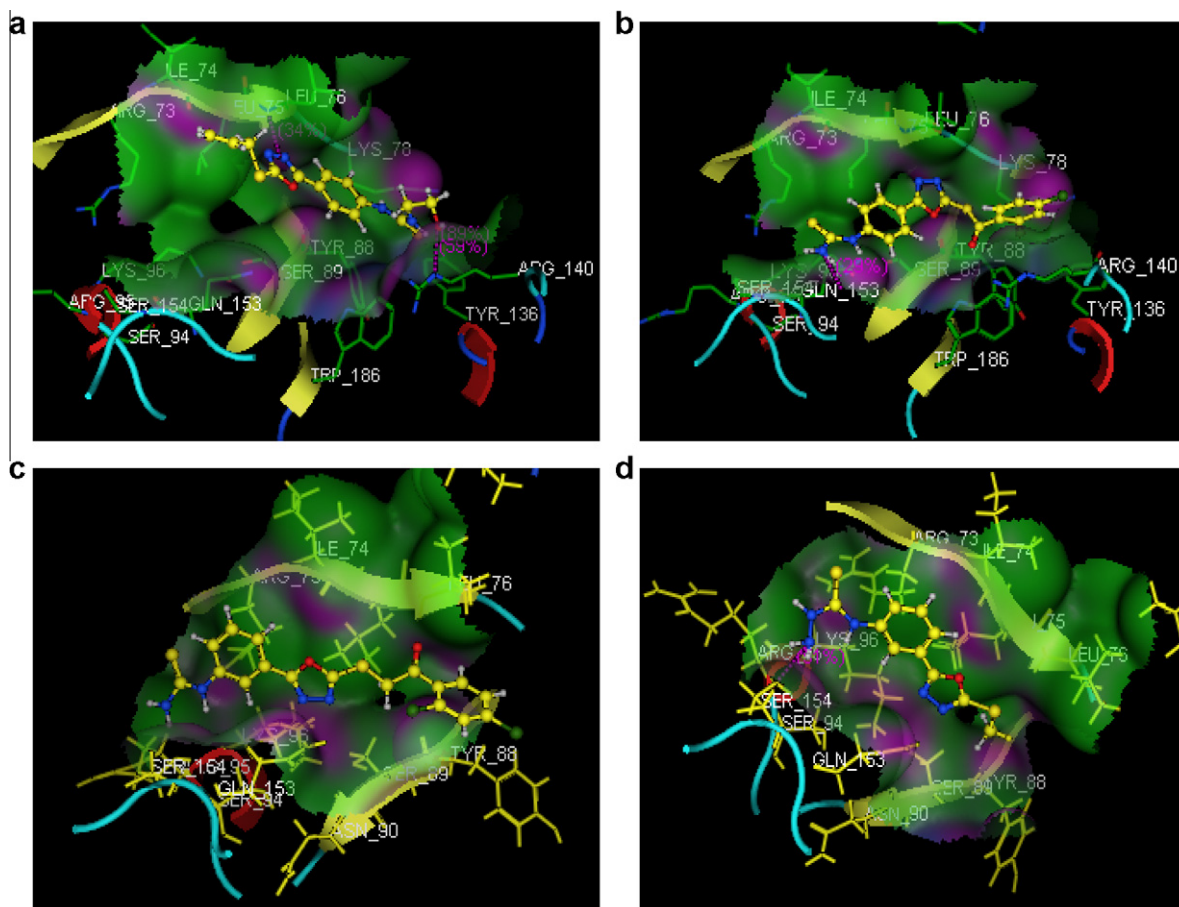


Figure 3. Docking of compounds **33** (a), **31** (b), **60** (c) and **20** (d) into the active site of protein Rv1155 from *Mycobacterium tuberculosis*. H-atoms of protein are not shown for clarity.

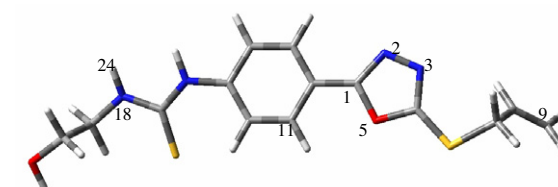
Arg73, Gln153, Ser154, Tyr88, Ile74, and Leu76 (Fig. 3c). The difference in its binding mode appears to be the reason behind the difference in binding affinity and, subsequently, in activities of compounds **33** (binding energy = -16.23 kcal/mol; docking energy = -19.95 kcal/mol) and **60** (binding energy = -10.35 kcal/mol; docking energy = -11.10 kcal/mol). The difference in binding mode may be attributed to the electronegative nature of carbonyl group, which favors an orientation that enables hydrogen bonding between the $-C=O$ group and Leu76. Docking of the inactive compound **20** showed favorable hydrogen bonding interactions between its NH_2 -group and Ile74 of the protein (Fig. 3d). According to the docking results, compound **20** (binding energy = -10.86 kcal/mol; docking energy = -12.06 kcal/mol) exhibits a binding mode similar to that of compound **60**.

From all the said it follows that binding modes for active and inactive compounds are different. Inactive compounds can be either rejected by the receptor or binded but with its other aminoacids then those that bind with active compounds. Binding affinities of inactive compounds are characterized by very low values in this case.

4.2. Analysis of pharmacophores and anti-pharmacophores

To form the basis of the system for the antituberculosis activity prediction, the compound **33** with the highest activity was taken as a template for the comparison first of all. In Figure 4, a submatrix of this template ETMC (i.e., its ETSC) is given, which corresponds to one of the pharmacophores revealed (namely, to Ph_1).

The given Ph_1 pharmacophore consists of eight atoms located in different parts of the template. The nitrogen atom N_{18} has a high



№33

C ₁	N ₂	N ₃	O ₅	C ₉	C ₁₁	N ₁₈	H ₂₄
0.01	1.58	2.18	1.05	7.12	2.48	6.68	7.59
	-0.07	1.26	2.25	6.75	3.77	7.87	8.81
		-0.11	1.08	5.46	4.60	8.87	9.74
			-0.11	6.13	2.86	7.08	7.90
				-0.18	8.95	12.92	13.63
					-0.07	4.23	5.29
						-0.32	0.88
							0.26

Figure 4. Submatrix (ETSC) and corresponding structure of the Ph_1 pharmacophore (template active compound **33**).

negative charge $q = -0.32e$; negative charges are concentrated on the atoms N_3 , O_5 , C_9 , N_2 , and C_{11} , as well. The charge on the C_1 carbon atom is close to zero. The rest of pharmacophores were found analogously, and the probabilities of their realization (P_a) in the class of active compounds varied in the limits of 0.80–0.90.

To determine anti-pharmacophores, ETMCs of several inactive compounds were taken as templates for the comparison with the rest of compounds. ETSC that corresponds to the Aph_1 anti-pharmacophore is given in Figure 4 along with the structure of

the corresponding template from which all anti-pharmacophores have been found.

As seen from Figure 5, APh₁ (found from the inactive compound **60** as a template) consists of atoms C₉, C₁₁, C₂₀, N₂₃, O₂₆, and Cl₂₇. Thus, a set of pharmacophores and anti-pharmacophores was calculated by the ETM relative to the series under study. Both groups of molecular fragments formed the basis of our system for the prediction of anti-mycobacterial activity against *M. tuberculosis* H37Rv.

The statistical characteristics of five pharmacophores (Ph_i) and five anti-pharmacophores (APh_i) entering the forecasting system, are given in Table 2. Figure 6 shows the frequencies of two pharmacophores, Ph₁ and Ph₂, and two anti-pharmacophores, APh₁ and APh₂, occurrence in the compounds studied and corresponding values of their activities.

As seen from Figure 6, pharmacophores appear with high frequencies in the class of active compounds, and they are practically absent in the class of inactive compounds. In a similar way, maximal values are observed for the frequencies of APh₁ and APh₂ appearance in the class of inactive compounds, while for Ph₁ and Ph₂ their frequencies are close to zero. In other words, the fragments found provide natural clustering of the series under study into two classes of compounds, namely, active and inactive ones. When comparing the structures of the pharmacophores and anti-pharmacophores, one can pay attention to the differences in their spatial and electron characteristics. Thus, when used together, both pharmacophores and anti-pharmacophores play definitely very important role for the activity prediction in the process of searching for a new potential drugs.

4.3. ETM-ANNs

The next step of the investigation was the ETM-ANNs combined approach application. A data set containing 82 molecules was taken. Seventy of the compounds were used for the model develop-

ment, while 12 randomly selected compounds were used for the model validation. For the mentioned training set and test set, 170 fragments were selected from the ETM study. The ASNNs recognized correctly 90.1%, or 65 from 70 compounds, for the training set and 92.0%, or 11 compounds from 12, for the test set (Table 3). The importance of the detected fragments for the antitubercular activity demonstration was evaluated as the result of using pruning methods at the last step of the algorithm.

The most part of the ETMC fragments were found to be nonsignificant for the system of prognosis and eliminated by the pruning algorithms. As a result, only three ETMC fragments from 250 selected previously by the experts from all fragments found appeared to be the most important ones. By this, ASNNs classified correctly 90.4%, or 67 compounds from 70 ones, in the training set and 92.0%, or 11 from 12 compounds, in the test set (Table 2).

As known, the highest occupied molecular orbital (HOMO) and the lowest unoccupied molecular orbital (LUMO), called also *frontier orbitals*, play an important role in the donor-acceptor interaction of a substance with the corresponding receptor. Analysis of HOMOs for the compounds containing Ph₁–Ph₅ and APh₁–APh₅ has shown that atoms with the highest values of the atomic orbital coefficients are mainly those atoms that form the pharmacophores. The HOMO orbitals are shown in Figure 7.

HOMO orbital for the template compound **33** consists of orbitals of those atoms that form aminosulfonyl group and, partially, phenyl and pyrazole rings. The most part of atoms representing Ph₁ are exactly those that deposit considerably to the HOMO orbitals. Similar situation can be observed in the case of template compounds **35**–**37**. In contrast to Ph₁, HOMO orbital of APh₁ consists of carbon atoms entering the phenyl ring and all atoms of monosubstituted thiourea group. All the said suggests an important role of these atoms in the substrate-receptor interaction.

5. Conclusion

Peculiarities of conformational and electron structures of compounds belonging to a large series of different 5-aryl-2-thio-1,3,4-thiadiazole derivatives which possess anti-mycobacterial activity against *M. tuberculosis* H37Rv have been studied. The results of the study are in agreement with data obtained by other researchers relative to the same classes of compounds. A system for the antituberculosis activity prediction was developed on the base of pharmacophores and anti-pharmacophores found in the process of this study. The system allows for the effective screening of active compounds and design of potent drugs.

The results of the ETM-ANNs application to the test sample show that 90% of the compounds taken are classified correctly (Table 2). Obviously, the immediate prediction done on the base of the ETM can give much higher percentage. To assess the activity of a molecule, the ETM-ANN uses a set of pharmacophores and anti-pharmacophores that have been found from a few different template compounds. For this reason, the percentage of test compounds that are correctly recognized with the help of ETM-ANN after training by the targets can sometimes be lower than the percent of test compounds correctly recognized after immediate results of ETM, that

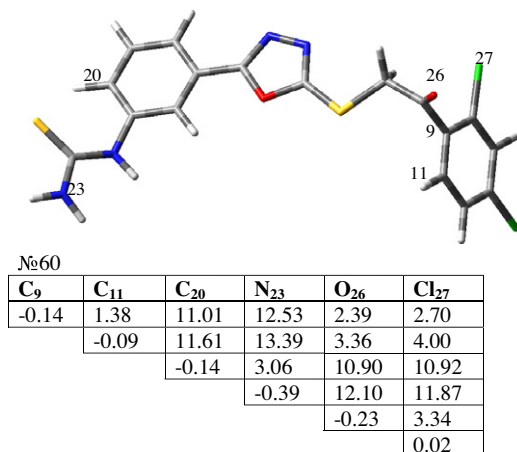


Figure 5. Submatrix (ETSC) and corresponding structure of the APh₁ antipharmacophore (the template compound **60**).

Table 2

Statistical characteristics for some of pharmacophores (Ph_i) and anti-pharmacophores (APh_i) calculated by ETM

Type of pharmacophore (template compound)	P_a	P_{ia}	Type of antipharmacophore (template compound)	P_a	P_{ia}
Ph ₁ (33)	0.90	0.10	APh ₁ (59)	0.07	0.93
Ph ₂ (35)	0.87	0.13	APh ₂ (44)	0.09	0.91
Ph ₃ (36)	0.85	0.15	APh ₃ (60)	0.13	0.87
Ph ₄ (37)	0.83	0.17	APh ₄ (49)	0.08	0.92
Ph ₅ (32)	0.80	0.20	APh ₅ (61)	0.10	0.90

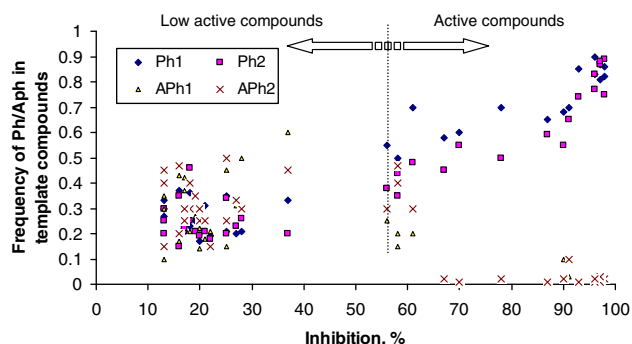


Figure 6. Frequency of the pharmacophores' (antipharmacophore's) occurrences in the compounds studied.

Table 3
The ETM-ANNs results based on data obtained from the pharmacophores set

	WD ^a number	All pharmacophores	
		Molecule	
		Amount	Predicted (%)
Training set	250	70	65 (90.1)
Test set	250	12	11 (92.0)
<i>Pharmacophores selected by pruning methods</i>			
Training set	10	70	67 (90.4)
Test set	10	12	11 (92.0)

^a WD_s, weight descriptors.

is, from the set of pharmacophores calculated for a single target compound.

The work on the volume of the set of possible pharmacophores/anti-pharmacophores reduction is an expert's work and is tedious enough. Unfortunately, it cannot be automated completely, and the expert's participation at this stage is obligatory. Neural networks can improve the results of this work as to finding the most significant activity fragments. Moreover, they can be trained to predict activities of new potent preparations, and after this they can be purposefully used by nonexperts, too.

The most active compounds dock well in the active site of the related enzymes. Inhibitory activity of the most potent compounds is explained mostly by hydrogen bonding and either electrostatic or π - π interactions within the active site of the enzyme. Hydrophilic and steric requirements are also very important factors in terms of SAR. Thus, this study can be a good starting point to improve the design of novel class of molecules possessing antituberculosis activity.

6. Experimental part

Solvents and commercially available reagents were purchased from Aldrich (Germany), Across (Belgium), and Lancaster (Great

Britain). Thin-layer chromatography was carried out on Merck aluminum sheets, silica gel 60 F_{254} . Column chromatography was performed on Fluka silica gel 60, 70–230 mesh. Melting points were determined on a Boëtius melting point apparatus (PHMK, VEB Wägetechnik Rapido, Radebeul, Germany) and are uncorrected. IR spectra were acquired on apparatus 'Perkin-Elmer Spectrum 100 FTIR'. ^1H NMR spectra were acquired on a Bruker Avance III 400 spectrometer operating at 400.13 MHz for ^1H . Chemical shifts δ are given in ppm referring to the signal center using the solvent peaks for reference: DMSO- d_6 2.50 ppm.

6.1. Precursors of compounds 3–82

1,3,4-Oxadiazoles **1**, **2** were prepared according to a known procedure.²⁷

6.1.1. 5-(4-Isothiocyanatophenyl)-1,3,4-oxadiazole-2-thiol (**1**)

Yield: 90%, mp: 197–199 °C. IR: 1612 (C=N), 2040 (NCS), 3066 (SH) cm^{-1} ; ^1H NMR (δ ppm, DMSO- d_6 , 400 MHz): 3.11 (s, 1H, SH), 7.88 (d, 2H, J = 8.94 Hz, Ar), 7.02 (d, 2H, J = 8.94 Hz, Ar). Anal. Calcd for $\text{C}_9\text{H}_5\text{N}_3\text{OS}_2$ (MW 235.29): C, 45.94; H, 2.14; N, 17.86. Found: C, 45.87; H, 2.17; N, 17.92.

6.1.2. 8.1.2.5-(3-Isothiocyanatophenyl)-1,3,4-oxadiazole-2-thiol (**2**)

Yield: 85%, mp: 138–140 °C. IR: 1615 (C=N), 2105 (NCS), 3083 (SH) cm^{-1} ; ^1H NMR (δ ppm, DMSO- d_6 , 400 MHz): 7.48–8.1 (m, 4H, Ar), 10.8 (s, 1H, SH). Anal. Calcd for $\text{C}_9\text{H}_5\text{N}_3\text{OS}_2$ (MW 235.29): C, 45.94; H, 2.14; N, 17.86. Found: C, 45.88; H, 2.18; N, 17.82.

6.2. General procedure for the synthesis of S-substituted 1,3,4-oxadiazoles 12–19, 48–55

To the stirred solution of 1,3,4-oxadiazole (4.2 mmol) and triethylamine (0.42 g, 4.2 mmol) in acetone (20 ml), one-portion solution of ω -phenacyl bromide (4.6 mmol) in acetone (5 ml) was added at room temperature. The reaction mixture was stirred for 2 h at room temperature (TLC control). The precipitate formed was filtered and washed with water and acetone. The same method was used for allyl bromide, benzyl chloride, methyl iodide.

6.2.1. 5-(4-Isothiocyanatophenyl)-2-methylsulfanyl-1,3,4-oxadiazole (**12**)

Yield: 90%, mp: 113–114 °C. IR: 1195 (SCH₃), 1456 (C=N), 2230 (NCS) cm^{-1} ; ^1H NMR (δ ppm, DMSO- d_6 , 400 MHz): 2.81 (s, 3H, Me), 7.48–7.97 (m, 4H, Ar). Anal. Calcd for $\text{C}_{10}\text{H}_7\text{N}_3\text{OS}_2$ (MW 249.31): C, 48.17; H, 2.83; N, 16.85. Found: C, 48.21; H, 2.78; N, 16.89.

6.2.2. 2-(4-Pyridylmethylsulfanyl)-5-(4-isothiocyanatophenyl)-1,3,4-oxadiazole (**13**)

To the stirred at rt solution of 2-mercapto-5-(4-isothiocyanatophenyl)-1,3,4-oxadiazole (1.41 g, 6 mmol) and triethylamine (1.21 g, 12 mmol) in acetone (30 ml), one-portion suspension of 4-chloromethylpyridine hydrochloride (1.0 g, 6.1 mmol) in acetone

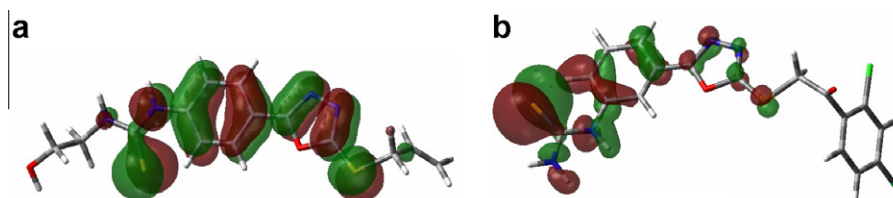


Figure 7. A three-dimensional view of HOMO orbitals for template compounds **33** (a) and **60** (b).

(10 ml) was added in. The reaction mixture was refluxed for 2 h (TLC control). When the reaction was completed, acetone was evaporated under reduced pressure, precipitate was suspended with water, filtered, washed with water and acetone.

Yield: 80%, mp: 151–152 °C. IR: 1600 (C=N), 2096 (NCS), 2591 (SCH₂) cm⁻¹; ¹H NMR (δ ppm, DMSO-*d*₆, 400 MHz): 4.51 (s, 2H, CH₂), 7.43–8.58 (m, 8H, Ar). Anal. Calcd for C₁₅H₁₀N₄OS₂ (MW 326.40): C, 55.20; H, 3.09; N, 17.17. Found: C, 55.25; H, 3.11; N, 17.21.

6.2.3. 2-Benzylsulfanyl-5-(4-isothiocyanatophenyl)-1,3,4-oxadiazole (14)

Yield: 81%, mp: 139–141 °C. IR: 1603 (C=N), 2098 (NCS), 2724 (SCH₂) cm⁻¹; ¹H NMR (δ ppm, DMSO-*d*₆, 400 MHz): 4.51 (s, 2H, CH₂), 7.23–8.11 (m, 9H, Ar). Anal. Calcd for C₁₆H₁₁N₃OS₂ (MW 325.41): C, 59.06; H, 3.41; N, 12.91. Found: C, 59.11; H, 3.44; N, 12.96.

6.2.4. 2-(2-pyrimidinylsulfanyl)-5-(4-isothiocyanatophenyl)-1,3,4-oxadiazole (15)

Suspension of 2-mercapto-5-(4-isothiocyanatophenyl)-1,3,4-oxadiazole **1** (1.17 g, 5 mmol) and K₂CO₃ (1.4 g, 10 mmol) in DMF (10 ml) was stirred during 5 min at rt, then solution of 2-chloropyrimidine (0.57 g, 5 mmol) in DMF (5 ml) was added. The reaction mixture was stirred for 3 h at 130 °C (TLC control). After this period, the reaction mixture was cooled to rt, water (50 ml) was added, and precipitate formed was filtered, washed with water, dried and recrystallized from ethanol.

Yield: 65%, mp: 173–175 °C. IR: 1554 (C=N), 2090 (NCS) cm⁻¹; ¹H NMR (δ ppm, DMSO-*d*₆, 400 MHz): 7.33–8.65 (m, 7H, Ar). Anal. Calcd for C₁₃H₇N₅OS₂ (MW 313.36): C, 49.83; H, 2.25; N, 22.35. Found: C, 49.85; H, 2.31; N, 22.38.

6.2.5. 1-(4-Fluorophenyl)-2-[5-(4-isothiocyanatophenyl)-1,3,4-oxadiazol-2-ylsulfanyl]-1-ethanone (16)

Yield: 91%, mp: 183–185 °C. IR: 1585 (C=N), 1675 (C=O), 2113 (NCS), 2605 (SCH₂) cm⁻¹; ¹H NMR (δ ppm, DMSO-*d*₆, 400 MHz): 5.19 (s, 2H, CH₂), 7.42–7.84 (m, 8H, Ar). Anal. Calcd for C₁₇H₁₀FN₃O₂S₂ (MW 371.41): C, 54.97; H, 2.71; N, 11.31. Found: C, 54.92; H, 2.74; N, 11.37.

6.2.6. 2-[5-(4-isothiocyanatophenyl)-1,3,4-oxadiazol-2-ylsulfanyl]-1-phenyl-1-ethanone (17)

Yield: 78%, mp: 168–170 °C. IR: 1594 (C=N), 1676 (C=O), 2114 (NCS), 2725 (SCH₂) cm⁻¹; ¹H NMR (δ ppm, DMSO-*d*₆, 400 MHz): 4.99 (s, 2H, CH₂), 7.24–7.68 (m, 5H, Ar), 7.91–8.12 (m, 4H, Ar). Anal. Calcd for C₁₇H₁₁N₃O₂S₂ (MW 353.42): C, 57.77; H, 3.14; N, 11.89. Found: C, 57.73; H, 3.16; N, 11.94.

6.2.7. 1-(2,4-Dichlorophenyl)-2-[5-(4-isothiocyanatophenyl)-1,3,4-oxadiazol-2-ylsulfanyl]-1-ethanone (18)

Yield: 83%, mp: 169–170 °C. IR: 1517 (C=N), 1664 (C=O), 2135 (NCS), 2724 (SCH₂) cm⁻¹; ¹H NMR (δ ppm, DMSO-*d*₆, 400 MHz): 4.87 (s, 2H, CH₂), 7.52–8.08 (m, 7H, Ar). Anal. Calcd for C₁₇H₉Cl₂N₃O₂S₂ (MW 422.31): C, 48.35; H, 2.15; N, 9.95. Found: C, 48.39; H, 2.19; N, 9.92.

6.2.8. 2-Allylsulfanyl-5-(4-isothiocyanatophenyl)-1,3,4-oxadiazole (19)

Yield: 87%, mp: 119–120 °C. IR: 1603 (C=N), 2108 (NCS), 2566 (SCH₂) cm⁻¹; ¹H NMR (δ ppm, DMSO-*d*₆, 400 MHz): 3.98 (d, 2H, J = 6.76 Hz, CH₂-CH), 5.10–5.46 (m, 2H, CH₂=CH), 5.75–6.17 (m, 1H, CH=CH₂), 7.63 (d, 2H, J = 8.4 Hz, Ar), 7.98 (d, 2H, J = 8.4 Hz, Ar). Anal. Calcd for C₁₂H₉N₃OS₂ (MW 275.35): C, 52.34; H, 3.29; N, 15.26. Found: C, 52.36; H, 3.29; N, 15.28.

6.2.9. 5-(3-Isothiocyanatophenyl)-2-phenylethylsulfanyl-1,3,4-oxadiazole (48)

Yield: 84%, mp: 59–61 °C. IR: 1621 (C=N), 2134 (NCS), 2789 (SCH₂) cm⁻¹; ¹H NMR (δ ppm, DMSO-*d*₆, 400 MHz): 3.08 (t, 2H, J = 7.97 Hz, CH₂S), 3.56 (t, 2H, J = 7.97 Hz, CH₂Ar), 7.15–7.34 (m, 5H, Ar), 7.58–7.98 (m, 4H, Ar). Anal. Calcd for C₁₇H₁₃N₃OS₂ (MW 339.43): C, 60.15; H, 3.86; N, 12.38. Found: C, 60.21; H, 3.89; N, 12.42.

6.2.10. 2-Benzylsulfanyl-5-(3-isothiocyanatophenyl)-1,3,4-oxadiazole (49)

Yield: 88%, mp: 80–81 °C. IR: 1640 (C=N), 2036 (NCS), 2720 (SCH₂) cm⁻¹; ¹H NMR (δ ppm, DMSO-*d*₆, 400 MHz): 4.59 (s, 2H, CH₂), 7.27–7.98 (m, 9H, Ar). Anal. Calcd for C₁₆H₁₁N₃OS₂ (MW 325.41): C, 59.06; H, 3.41; N, 12.91. Found: C, 59.11; H, 3.44; N, 12.87.

6.2.11. 2-[5-(3-Isothiocyanatophenyl)-1,3,4-oxadiazol-2-ylsulfanyl]-1-(2-naphthyl)-1-ethanone (50)

Yield: 78%, mp: 175–177 °C. IR: 1498 (C=N), 1673 (C=O), 2230 (NCS), 2879 (SCH₂) cm⁻¹; ¹H NMR (δ ppm, DMSO-*d*₆, 400 MHz): 5.33 (s, 2H, CH₂), 7.50–8.22 (m, 11H, Ar). Anal. Calcd for C₂₁H₁₃N₃O₂S₂ (MW 403.04): C, 62.51; H, 3.25; N, 10.41. Found: C, 62.55; H, 3.27; N, 10.48.

6.2.12. 1-(4-Bromophenyl)-2-[5-(3-isothiocyanatophenyl)-1,3,4-oxadiazol-2-ylsulfanyl]-1-ethanone (51)

Yield: 76%, mp: 165–167 °C. IR: 1515 (C=N), 1675 (C=O), 2176 (NCS), 2770 (SCH₂) cm⁻¹; ¹H NMR (δ ppm, DMSO-*d*₆, 400 MHz): 5.17 (s, 2H, CH₂), 7.61–8.15 (m, 8H, Ar). Anal. Calcd for C₁₇H₁₀BrN₃O₂S₂ (MW 432.31): C, 47.23; H, 2.33; N, 9.72. Found: C, 47.27; H, 2.27; N, 9.78.

6.2.13. 1-(2,4-Dichlorophenyl)-2-[5-(3-isothiocyanatophenyl)-1,3,4-oxadiazol-2-ylsulfanyl]-1-ethanone (52)

Yield: 81%, mp: 141–143 °C. IR: 1540 (C=N), 1677 (C=O), 2132 (NCS), 2667 (SCH₂) cm⁻¹; ¹H NMR (δ ppm, DMSO-*d*₆, 400 MHz): 5.02 (s, 2H, CH₂), 7.54–7.99 (m, 7H, Ar). Anal. Calcd for C₁₇H₉Cl₂N₃O₂S₂ (MW 422.31): C, 48.35; H, 2.15; N, 9.95. Found: C, 48.39; H, 2.19; N, 9.92.

6.2.14. 2-Allylsulfanyl-5-(3-isothiocyanatophenyl)-1,3,4-oxadiazole (53)

Yield: 70%, mp: 43–45 °C. IR: 1560 (C=N), 2134 (NCS), 2556 (SCH₂) cm⁻¹; ¹H NMR (δ ppm, DMSO-*d*₆, 400 MHz): 3.94 (d, 2H, J = 6.74 Hz, CH₂-CH), 5.12–5.44 (m, 2H, CH₂=CH), 5.85–6.18 (m, 1H, CH=CH₂), 7.47–7.87 (m, 4H, Ar). Anal. Calcd for C₁₂H₉N₃OS₂ (MW 275.35): C, 52.34; H, 3.29; N, 15.26. Found: C, 52.36; H, 3.32; N, 15.33.

6.2.15. 1-(4-Fluorophenyl)-2-[5-(3-isothiocyanatophenyl)-1,3,4-oxadiazol-2-ylsulfanyl]-1-ethanone (54)

Yield: 79%, mp: 133–134 °C. IR: 1587 (C=N), 1676 (C=O), 2245 (NCS), 2600 (SCH₂) cm⁻¹; ¹H NMR (δ ppm, DMSO-*d*₆, 400 MHz): 5.19 (s, 2H, CH₂), 7.42–7.92 (m, 8H, Ar). Anal. Calcd for C₁₇H₁₀FN₃O₂S₂ (MW 371.41): C, 54.97; H, 2.71; N, 11.31. Found: C, 54.92; H, 2.75; N, 11.38.

6.2.16. 1-(4-Chlorophenyl)-2-[5-(3-isothiocyanatophenyl)-1,3,4-oxadiazol-2-ylsulfanyl]-1-ethanone (55)

Yield: 87%, mp: 165–166 °C. IR (Nujol) 1435 (C=N), 1678 (C=O), 2120 (NCS), 2680 (SCH₂) cm⁻¹; ¹H NMR (δ ppm, DMSO-*d*₆, 400 MHz): 5.16 (s, 2H, CH₂), 7.51–8.13 (m, 8H, Ar). Anal. Calcd for C₁₇H₁₀ClN₃O₂S₂ (MW 387.86): C, 52.64; H, 2.60; N, 10.83. Found: C, 52.69; H, 2.68; N, 10.89.

6.3. General procedure for the synthesis of amines 3–11, 20–47, 56–82

To the solution of 1,3,4-oxadiazole (7 mmol) in benzene (30 ml), the corresponding amine (8 mmol) was added. The reaction mixture was refluxed for 3 h (TLC control), cooled to rt and precipitate was filtered, washed with benzene, and dried.

6.3.1. Methylamino-4-(5-sulfanyl-1,3,4-oxadiazol-2-yl) anilino-methanethione (3)

Yield: 70%, mp: 246 °C. IR: 1315 (C=S), 1655 (C=N), 2678 (SH), 3089 (NH) cm^{-1} ; ^1H NMR (δ ppm, DMSO- d_6 , 400 MHz): 2.99 (d, 3H, J = 4.00 Hz, Me), 7.74 (d, 2H, J = 9.2 Hz, Ar), 7.79 (d, 2H, J = 9.2 Hz, Ar), 7.86 (s, 1H, NHMe), 9.76 (s, 1H, NHAr), 14.37 (s, 1H, SH). Anal. Calcd for $\text{C}_{10}\text{H}_{10}\text{N}_4\text{OS}_2$ (MW 266.34): C, 45.09; H, 3.78; N, 21.04. Found: C, 45.14; H, 3.82; N, 21.11.

6.3.2. Amino-4-(5-sulfanyl-1,3,4-oxadiazol-2-yl) anilino-methanethione (4)

Yield: 72%, mp: 245–246 °C. IR: 1324 (C=S), 1622 (C=N), 2732 (SH), 3374 (NH $_2$) cm^{-1} ; ^1H NMR (δ ppm, DMSO- d_6 , 400 MHz): 7.40–7.84 (m, 6H, Ar, NH $_2$), 10.01 (s, 2H, NH, SH). Anal. Calcd for $\text{C}_9\text{H}_8\text{N}_4\text{OS}_2$ (MW 252.32): C, 42.84; H, 3.20; N, 22.20. Found: C, 42.92; H, 3.25; N, 22.31.

6.3.3. Ethylamino-4-(5-sulfanyl-1,3,4-oxadiazol-2-yl)anilino-methanethione (5)

Yield: 75%, mp: 208–210 °C. IR: 1323 (C=S), 1547 (C=N), 2634 (SH), 3059 (NH) cm^{-1} ; ^1H NMR (δ ppm, DMSO- d_6 , 400 MHz): 1.20 (t, 3H, J = 7.2 Hz, Me), 3.53 (t, 2H, J = 6.00 Hz, CH $_2$), 7.78 (d, 2H, J = 10.00 Hz, Ar), 7.80 (d, 2H, J = 10.00 Hz, Ar), 8.01 (s, 1H, NHCH $_2$), 9.87 (s, 1H, NHAr), 14.38 (s, 1H, SH). Anal. Calcd for $\text{C}_{11}\text{H}_{12}\text{N}_4\text{OS}_2$ (MW 280.37): C, 47.12; H, 4.31; N, 19.98. Found: C, 47.18; H, 4.37; N, 19.88.

6.3.4. Piperidino-4-(5-sulfanyl-1,3,4-oxadiazol-2-yl) anilino-methanethione (6)

Yield: 68%, mp: 182–183 °C. IR: 1355 (C=S), 1546 (C=N), 2635 (SH), 3090 (NH) cm^{-1} ; ^1H NMR (δ ppm, DMSO- d_6 , 400 MHz): 1.71 (s, 6H, 3CH $_2$), 3.88 (s, 4H, N(CH $_2$) $_2$), 7.49 (d, 2H, J = 8.6 Hz, Ar), 7.79 (d, 2H, J = 8.6 Hz, Ar), 9.36 (s, 1H, NH), 14.35 (s, 1H, SH). Anal. Calcd for $\text{C}_{14}\text{H}_{16}\text{N}_4\text{OS}_2$ (MW 320.43): C, 52.48; H, 5.03; N, 17.48. Found: C, 52.52; H, 5.10; N, 17.53.

6.3.5. 2-Hydroxyethylamino-4-(5-sulfanyl-1,3,4-oxadiazol-2-yl) anilino-methanethione (7)

Yield: 92%, mp: 190–191 °C. IR: 1275 (C=S), 1554 (C=N), 2734 (SH), 3441 (OH) cm^{-1} ; ^1H NMR (δ ppm, DMSO- d_6 , 400 MHz): 3.58–3.67 (m, 4H, (CH $_2$) $_2$ NH), 4.79 (s, 1H, OH), 7.78–8.09 (m, 5H, Ar, NHCH $_2$), 9.97 (s, 2H, NHAr, SH). Anal. Calcd for $\text{C}_{11}\text{H}_{12}\text{N}_4\text{O}_2\text{S}_2$ (MW 296.37): C, 44.58; H, 4.08; N, 18.90. Found: C, 44.64; H, 4.14; N, 18.97.

6.3.6. N-(4-(5-Mercapto-1,3,4-oxadiazol-2-yl)phenyl)-2,2-dimethylhydrazinecarbo thioamide (8)

Yield: 84%, mp: 218–220 °C. IR: 1334 (C=S), 1546 (C=N), 2650 (SH), 3078 (NH) cm^{-1} ; ^1H NMR (δ ppm, DMSO- d_6 , 400 MHz): 2.18 (s, 6H, 2Me), 7.38 (d, 2H, J = 8.4 Hz, Ar), 7.56 (d, 2H, J = 8.4 Hz, Ar), 9.13 (s, 1H, NHN), 9.75 (s, 1H, NHAr), 14.05 (s, 1H, SH). Anal. Calcd for $\text{C}_{11}\text{H}_{12}\text{N}_4\text{OS}_2$ (MW 280.37): C, 47.12; H, 4.31; N, 19.98. Found: C, 47.14; H, 4.37; N, 19.89.

6.3.7. 4-(5-Sulfanyl-1,3,4-oxadiazol-2-yl)anilino-4-toluidinome-thanethione (9)

Yield: 88%, mp: 178–180 °C. IR: 1440 (C=S), 1645 (C=N), 2570 (SH), 3058 (NH) cm^{-1} ; ^1H NMR (δ ppm, DMSO- d_6 , 400 MHz): 2.33

(s, 3H, Me), 7.15 (d, 2H, J = 7.6 Hz, MeC $_6$ H $_4$ N), 7.32 (d, 2H, J = 7.6 Hz, MeC $_6$ H $_4$ N), 7.78 (d, 2H, J = 8.40 Hz, Ar), 7.81 (d, 2H, J = 8.40 Hz, Ar), 9.78 (s, 1H, NHp-tolyl), 9.84 (s, 1H, NHAr), 14.45 (s, 1H, SH). Anal. Calcd for $\text{C}_{16}\text{H}_{14}\text{N}_4\text{OS}_2$ (MW 342.44): C, 56.12; H, 4.12; N, 16.36. Found: C, 56.17; H, 4.17; N, 16.42.

6.3.8. Allylamino-4-(5-sulfanyl-1,3,4-oxadiazol-2-yl) anilino-methanethione (10)

Yield: 73%, mp: 185–187 °C. IR: 1330 (C=S), 1640 (C=N), 2657 (SH), 3090 (NH) cm^{-1} ; ^1H NMR (δ ppm, DMSO- d_6 , 400 MHz): 4.17 (s, 2H, CH $_2$ N), 5.13 (d, 1H, J = 10.00 Hz, CH $_2$ =CH), 5.24 (d, 1H, J = 17.20 Hz, CH $_2$ =CH), 5.87–5.96 (m, 1H, CH=CH $_2$), 7.52–7.98 (m, 5H, Ar, NHCH $_2$), 9.76 (s, 1H, NHAr), 14.26 (s, 1H, SH). Anal. Calcd for $\text{C}_{12}\text{H}_{12}\text{N}_4\text{OS}_2$ (MW 292.38): C, 49.29; H, 4.14; N, 19.16. Found: C, 49.32; H, 4.08; N, 19.23.

6.3.9. Hydrazino-4-(5-sulfanyl-1,3,4-oxadiazol-2-yl) anilino-methanethione (11)

Yield: 68%, mp: 226–227 °C. IR: 1341 (C=S), 1616 (C=N), 2641 (SH), 3255 (NH $_2$) cm^{-1} ; ^1H NMR (δ ppm, DMSO- d_6 , 400 MHz): 7.83–7.95 (m, 4H, Ar), 9.27 (s, 1H, NHHNH $_2$), 9.94 (s, 1H, NHAr), 14.15 (s, 1H, SH). Anal. Calcd for $\text{C}_9\text{H}_9\text{N}_5\text{OS}_2$ (MW 267.33): C, 40.44; H, 3.39; N, 26.20. Found: C, 40.51; H, 3.43; N, 26.26.

6.3.10. Hydrazino-4-(5-methylsulfanyl-1,3,4-oxadiazol-2-yl) anilino-methanethione (20)

Yield: 74%, mp: 275 (dec) °C. IR: 1242 (SCH $_3$), 1475 (C=S), 1618 (C=N), 3450 (NH $_2$) cm^{-1} ; ^1H NMR (δ ppm, DMSO- d_6 , 400 MHz): 2.78 (s, 3H, Me), 7.85–7.99 (m, 4H, Ar), 9.21 (s, 1H, NHHNH $_2$), 9.98 (s, 1H, NHAr). Anal. Calcd for $\text{C}_{10}\text{H}_{11}\text{N}_5\text{OS}_2$ (MW 281.36): C, 42.69; H, 3.94; N, 24.89. Found: C, 42.53; H, 3.88; N, 24.94.

6.3.11. 4-(5-Methylsulfanyl-1,3,4-oxadiazol-2-yl)anilino-4-toluidinomethanethione (21)

Yield: 71%, mp: 198–200 °C. IR: 1179 (SCH $_3$), 1370 (C=S), 1632 (C=N), 3098 (NH) cm^{-1} ; ^1H NMR (δ ppm, DMSO- d_6 , 400 MHz): 2.34 (s, 3H, MeAr), 2.77 (s, 3H, SMe), 7.12 (d, 2H, J = 8.00 Hz, MeC $_6$ H $_4$ NH), 7.36 (d, 2H, J = 8.00 Hz, MeC $_6$ H $_4$ NH), 7.78 (d, 2H, J = 8.80 Hz, Ar), 7.88 (d, 2H, J = 8.80 Hz, Ar), 9.81 (s, 1H, NHp-tolyl), 9.89 (s, 1H, NHAr). Anal. Calcd for $\text{C}_{17}\text{H}_{16}\text{N}_4\text{OS}_2$ (MW 358.48): C, 57.28; H, 4.52; N, 15.72. Found: C, 57.33; H, 4.48; N, 15.81.

6.3.12. 4-(5-Methylsulfanyl-1,3,4-oxadiazol-2-yl) anilino-morpholinomethanethione (22)

Yield: 69%, mp: 160–162 °C. IR: 1234 (SCH $_3$), 1320 (C=S), 1631 (C=N), 3158 (NH) cm^{-1} ; ^1H NMR (δ ppm, DMSO- d_6 , 400 MHz): 2.77 (s, 3H, Me), 3.69 (t, 4H, J = 4.6 Hz, 2OCH $_2$), 3.92 (t, 4H, J = 4.6 Hz, N(CH $_2$) $_2$), 7.54 (d, 2H, J = 8.4 Hz, Ar), 7.87 (d, 2H, J = 8.4 Hz, Ar), 9.49 (s, 1H, NH). Anal. Calcd for $\text{C}_{14}\text{H}_{16}\text{N}_4\text{O}_2\text{S}_2$ (MW 336.43): C, 49.98; H, 4.79; N, 16.65. Found: C, 49.91; H, 4.82; N, 16.69.

6.3.13. 4-(5-Methylsulfanyl-1,3,4-oxadiazol-2-yl)anilino-4H-1,2,4-triazol-4-yl-amino methanethione (23)

Yield: 86%, mp: 139–140 °C. IR: 1197 (SCH $_3$), 1368 (C=S), 1647 (C=N), 3230 (NH) cm^{-1} ; ^1H NMR (δ ppm, DMSO- d_6 , 400 MHz): 2.80 (s, 3H, Me), 7.50 (d, 2H, J = 8.4 Hz, Ar), 7.79 (d, 2H, J = 8.4 Hz, Ar), 8.65 (s, 2H, Tr), 10.08 (s, 1H, NHAr), 10.78 (s, 1H, NHTr). Anal. Calcd for $\text{C}_{12}\text{H}_{11}\text{N}_7\text{OS}_2$ (MW 333.39): C, 43.23; H, 3.33; N, 29.41. Found: C, 43.27; H, 3.41; N, 29.52.

6.3.14. Amino-4-(5-methylsulfanyl-1,3,4-oxadiazol-2-yl) anilino-methanethione (24)

Yield: 81%, mp: 211–213 °C. IR: 1354 (SCH $_3$), 1368 (C=S), 1667 (C=N), 3640 (NH $_2$) cm^{-1} ; ^1H NMR (δ ppm, DMSO- d_6 , 400 MHz):

2.85 (s, 3H, Me), 7.19–8.05 (m, 6H, Ar, NH₂), 9.94 (s, 1H, NH). Anal. Calcd for C₁₀H₁₀N₄O₅S₂ (MW 266.34): C, 45.09; H, 3.78; N, 21.04. Found: C, 45.13; H, 3.83; N, 21.11.

6.3.15. 2-Hydroxyethylamino-4-(5-methylsulfanyl-1,3,4-oxadiazol-2-yl)anilinomethanethione (25)

Yield: 64%, mp: 140–141 °C. IR: 1340 (SCH₃), 1380 (C=S), 1635 (C=N), 3519 (OH) cm⁻¹; ¹H NMR (δ ppm, DMSO-*d*₆, 400 MHz): 2.78 (s, 3H, Me), 3.65 (s, 4H, (CH₂)₂NH), 4.83 (s, 1H, OH), 7.89–7.95 (m, 5H, Ar, NHCH₂), 9.91 (s, 1H, NHAr). Anal. Calcd for C₁₂H₁₄N₄O₅S₂ (MW 310.40): C, 46.43; H, 4.55; N, 18.05. Found: C, 46.47; H, 4.61; N, 18.12.

6.3.16. 2-Hydroxyethylamino-4-[5-(4-pyridylmethylsulfanyl)-1,3,4-oxadiazol-2-yl]anilinomethanethione (26)

Yield: 72%, mp: 168–169 °C. IR: 1475 (C=S), 1606 (C=N), 2727 (SCH₂), 3500 (OH) cm⁻¹; ¹H NMR (δ ppm, DMSO-*d*₆, 400 MHz): 3.53–3.58 (m, 4H, (CH₂)₂NH), 4.57 (s, 1H, OH), 4.87 (s, 2H, SCH₂), 7.35–8.03 (m, 9H, Ar, NHCH₂), 9.84 (s, 1H, NHAr). Anal. Calcd for C₁₇H₁₇N₅O₅S₂ (MW 387.48): C, 52.69; H, 4.42; N, 18.07. Found: C, 52.73; H, 4.46; N, 18.12.

6.3.17. 2-5-[4-Amino(thioxo)methylaminophenyl]-1,3,4-oxadiazol-2-ylsulfanyl-1-phenyl-1-ethanone (27)

Yield: 86%, mp: 207–209 °C. IR: 1468 (C=S), 1662 (C=N), 1677 (C=O), 3347 (NH₂) cm⁻¹; ¹H NMR (δ ppm, DMSO-*d*₆, 400 MHz): 5.18 (s, 2H, CH₂), 7.38–8.21 (m, 11H, Ar, NH₂), 9.93 (s, 1H, NH). Anal. Calcd for C₁₇H₁₄N₄O₂S₂ (MW 370.45): C, 55.12; H, 3.81; N, 15.12. Found: C, 55.17; H, 3.85; N, 15.17.

6.3.18. Amino-4-[5-(2-pyrimidinylsulfanyl)-1,3,4-oxadiazol-2-yl]anilinomethanethione (28)

Yield: 78%, mp: 214–215 °C. IR: 1372 (C=S), 1630 (C=N), 3150 (NH), 3320 (NH₂) cm⁻¹; ¹H NMR (δ ppm, DMSO-*d*₆, 400 MHz): 7.25–8.75 (m, 9H, Ar, NH₂), 9.92 (s, 1H, NH). Anal. Calcd for C₁₃H₁₀N₆O₅S₂ (MW 330.39): C, 47.26; H, 3.05; N, 25.44. Found: C, 47.29; H, 3.11; N, 25.48.

6.3.19. 1-(4-Fluorophenyl)-2-(5-[2-hydroxyethylamino(thioxo)methylamino]phenyl-1,3,4-oxadiazol-2-ylsulfanyl)-1-ethanone (29)

Yield: 85%, mp: 180–182 °C. IR: 1338 (C=S), 1541 (C=N), 1676 (C=O), 3225 (OH) cm⁻¹; ¹H NMR (δ ppm, DMSO-*d*₆, 400 MHz): 3.52–3.59 (m, 4H, (CH₂)₂NH), 4.88 (s, 1H, OH), 5.16 (s, 2H, SCH₂), 7.34–7.65 (m, 5H, Ar, NHCH₂), 8.07–8.25 (m, 4H, Ar), 9.84 (s, 1H, NHAr). Anal. Calcd for C₁₉H₁₇FN₄O₃S₂ (MW 432.49): C, 52.76; H, 3.96; N, 12.95. Found: C, 52.79; H, 3.92; N, 12.89.

6.3.20. Amino-4-(5-benzylsulfanyl-1,3,4-oxadiazol-2-yl)anilinomethanethione (30)

Yield: 77%, mp: 179–180 °C. IR: 1469 (C=S), 1656 (C=N), 2727 (SCH₂), 3330 (NH₂) cm⁻¹; ¹H NMR (δ ppm, DMSO-*d*₆, 400 MHz): 4.57 (s, 2H, CH₂), 6.98–8.05 (m, 11H, Ar, NH₂), 9.93 (s, 1H, NH). Anal. Calcd for C₁₆H₁₄N₄O₅S₂ (MW 342.44): C, 56.12; H, 4.12; N, 16.36. Found: C, 56.15; H, 4.17; N, 16.38.

6.3.21. 2-5-[4-Amino(thioxo)methylaminophenyl]-1,3,4-oxadiazol-2-ylsulfanyl-1-(2,4-dichlorophenyl)-1-ethanone (31)

Yield: 79%, mp: 170–171 °C. IR: 1477 (C=S), 1620 (C=N), 1664 (C=O), 3448 (NH₂) cm⁻¹; ¹H NMR (δ ppm, DMSO-*d*₆, 400 MHz): 5.01 (s, 2H, CH₂), 7.38–8.11 (m, 9H, Ar, NH₂), 9.93 (s, 1H, NH). Anal. Calcd for C₁₇H₁₂Cl₂N₄O₅S₂ (MW 439.34): C, 46.47; H, 2.75; N, 12.75. Found: C, 46.52; H, 2.79; N, 12.79.

6.3.22. 2-(5-[2-Hydroxyethylamino(thioxo)methylamino]phenyl-1,3,4-oxadiazol-2-ylsulfanyl)-1-phenyl-1-ethanone (32)

Yield: 73%, mp: 167–169 °C. IR: 1473 (C=S), 1544 (C=N), 1675 (C=O), 3254 (OH) cm⁻¹; ¹H NMR (δ ppm, DMSO-*d*₆, 400 MHz): 3.61 (s, 4H, (CH₂)₂NH), 4.72 (s, 1H, OH), 5.08 (s, 2H, SCH₂), 7.50–8.07 (m, 10H, Ar, NHCH₂), 9.82 (s, 1H, NHAr). Anal. Calcd for C₁₉H₁₈N₄O₃S₂ (MW 414.50): C, 55.05; H, 4.38; N, 13.52. Found: C, 55.12; H, 4.42; N, 13.54.

6.3.23. 4-(5-Allylsulfanyl-1,3,4-oxadiazol-2-yl)anilino-2-hydroxyethylaminomethane-thione (33)

Yield: 81%, mp: 121–122 °C. IR: 1313 (C=S), 1533 (C=N), 2726 (SCH₂), 3342 (OH) cm⁻¹; ¹H NMR (δ ppm, DMSO-*d*₆, 400 MHz): 3.54–3.59 (m, 4H, (CH₂)₂NH), 3.95 (d, 2H, *J* = 6.86 Hz, CH₂-CH), 4.91 (s, 1H, OH), 5.11–5.43 (m, 2H, CH₂=CH), 5.76–6.17 (m, 1H, CH=CH₂), 7.70–8.04 (m, 5H, Ar, NHCH₂), 9.97 (s, 1H, NHAr). Anal. Calcd for C₁₄H₁₆N₄O₂S₂ (MW 336.43): C, 49.98; H, 4.79; N, 16.65. Found: C, 49.93; H, 4.82; N, 16.71.

6.3.24. 4-(5-Benzylsulfanyl-1,3,4-oxadiazol-2-yl)anilino-2-hydroxyethylaminomethane-thione (34)

Yield: 84%, mp: 139–140 °C. IR: 1320 (C=S), 1611 (C=N), 2879 (SCH₂), 3345 (OH) cm⁻¹; ¹H NMR (δ ppm, DMSO-*d*₆, 400 MHz): 3.52–3.58 (m, 4H, (CH₂)₂NH), 4.57 (s, 1H, OH), 5.00 (s, 2H, SCH₂), 6.99–8.19 (m, 10H, Ar, NHCH₂), 9.83 (s, 1H, NHAr). Anal. Calcd for C₁₈H₁₈N₄O₂S₂ (MW 386.49): C, 55.94; H, 4.69; N, 14.50. Found: C, 55.97; H, 4.72; N, 14.54.

6.3.25. 4-(5-Allylsulfanyl-1,3,4-oxadiazol-2-yl)anilino-ami-nomethanethione (35)

Yield: 79%, mp: 173–174 °C. IR: 1347 (C=S), 1657 (C=N), 2729 (SCH₂), 3337 (NH₂) cm⁻¹; ¹H NMR (δ ppm, DMSO-*d*₆, 400 MHz): 3.94 (d, 2H, *J* = 6.81 Hz, CH₂-CH), 5.07–5.41 (m, 2H, CH₂=CH), 5.74–6.24 (m, 1H, CH=CH₂), 7.33–7.95 (m, 6H, Ar, NH₂), 10.05 (s, 1H, NH). Anal. Calcd for C₁₂H₁₂N₄O₅S₂ (MW 292.38): C, 49.29; H, 4.14; N, 19.16. Found: C, 49.32; H, 4.17; N, 19.21.

6.3.26. 1-(2,4-Dichlorophenyl)-2-(5-[2-hydroxyethylamino(thioxo)methylamino]phenyl-1,3,4-oxadiazol-2-ylsulfanyl)-1-ethanone (36)

Yield: 71%, mp: 163–164 °C. IR: 1469 (C=S), 1541 (C=N), 1674 (C=O), 3469 (OH) cm⁻¹; ¹H NMR (δ ppm, DMSO-*d*₆, 400 MHz): 3.55–3.58 (m, 4H, (CH₂)₂NH), 4.88 (s, 1H, OH), 5.01 (s, 2H, SCH₂), 7.25–8.01 (m, 8H, Ar, NHCH₂), 9.82 (s, 1H, NHAr). Anal. Calcd for C₁₉H₁₆Cl₂N₄O₃S₂ (MW 483.39): C, 47.21; H, 3.34; N, 11.59. Found: C, 47.26; H, 3.38; N, 11.63.

6.3.27. Amino-4-[5-(4-pyridylmethylsulfanyl)-1,3,4-oxadiazol-2-yl]anilinomethanethione (37)

Yield: 82%, mp: 203–204 °C. IR: 1473 (C=S), 1669 (C=N), 2742 (SCH₂), 3343 (NH₂) cm⁻¹; ¹H NMR (δ ppm, DMSO-*d*₆, 400 MHz): 4.55 (s, 2H, CH₂), 7.91–8.55 (m, 10H, Ar, NH₂), 9.93 (s, 1H, NH). Anal. Calcd for C₁₅H₁₃N₅O₅S₂ (MW 343.43): C, 52.46; H, 3.82; N, 20.39. Found: C, 52.49; H, 3.87; N, 20.43.

6.3.28. 2-Hydroxyethylamino-4-[5-(2-pyrimidinylsulfanyl)-1,3,4-oxadiazol-2-yl]anilinomethanethione (38)

Yield: 78%, mp: 188–189 °C. IR: 1379 (C=S), 1613 (C=N), 3182 (NH), 3462 (OH) cm⁻¹; ¹H NMR (δ ppm, DMSO-*d*₆, 400 MHz): 3.50–3.54 (m, 4H, (CH₂)₂NH), 4.89 (s, 1H, OH), 7.34–8.45 (m, 8H, Ar, NHCH₂), 9.83 (s, 1H, NHAr). Anal. Calcd for C₁₅H₁₄N₆O₅S₂ (MW 374.44): C, 48.11; H, 3.77; N, 22.44. Found: C, 48.15; H, 3.79; N, 22.48.

6.3.29. Allylamino-3-(5-sulfanyl-1,3,4-oxadiazol-2-yl) anilino-methanethione (39)

Yield: 71%, mp: 170–171 °C. IR: 1320 (C=S), 1634 (C=N), 2655 (SH), 3180 (NH) cm^{-1} ; ^1H NMR (δ ppm, DMSO- d_6 , 400 MHz): 3.90 (s, 2H, CH_2N), 5.16 (d, 1H, $J = 9.8$ Hz, $\text{CH}_2=\text{CH}$), 5.22 (d, 1H, $J = 16.80$ Hz, $\text{CH}_2=\text{CH}$), 5.79–6.20 (m, 1H, $\text{CH}=\text{CH}_2$), 7.48–7.86 (m, 5H, Ar, NHCH_2), 9.81 (s, 1H, NHAr), 14.22 (s, 1H, SH). Anal. Calcd for $\text{C}_{12}\text{H}_{12}\text{N}_4\text{OS}_2$ (MW 292.38): C, 49.29; H, 4.14; N, 19.16. Found: C, 49.33; H, 4.07; N, 19.24.

6.3.30. N-(3-(5-Mercapto-1,3,4-oxadiazol-2-yl)phenyl)-2-(propan-2-ylidene)hydrazine-carbothioamide (40)

Yield: 67%, mp: 203–205 °C. IR: 1483 (C=S), 1647 (C=N), 2720 (SH), 3223 (NH) cm^{-1} ; ^1H NMR (δ ppm, DMSO- d_6 , 400 MHz): 2.04 (s, 3H, Me), 2.07 (s, 3H, Me), 7.47 (t, 1H, $J = 8.00$ Hz, Ar), 7.68 (d, 1H, $J = 8.00$ Hz, Ar), 7.91 (d, 1H, $J = 8.00$ Hz, Ar), 8.27 (s, 1H, $J = 8.00$ Hz, Ar), 9.76 (s, 1H, NHN), 10.36 (s, 1H, NHAr), 14.44 (s, 1H, SH). Anal. Calcd for $\text{C}_{12}\text{H}_{13}\text{N}_5\text{OS}_2$ (MW 307.39): C, 46.89; H, 4.26; N, 22.78. Found: C, 46.97; H, 4.33; N, 22.85.

6.3.31. N-(3-(5-Mercapto-1,3,4-oxadiazol-2-yl)phenyl)-2-(1-phenylethylidene)hydrazine carbothioamide (41)

Yield: 75%, mp: 212–214 °C. IR: 1370 (C=S), 1647 (C=N), 2655 (SH), 3076 (NH) cm^{-1} ; ^1H NMR (δ ppm, DMSO- d_6 , 400 MHz): 2.43 (s, 3H, Me), 7.35–7.41 (m, 3H, Ar), 7.51 (t, 1H, $J = 8.00$ Hz, Ar), 7.72 (d, 1H, $J = 7.60$ Hz, Ar), 7.89 (d, 1H, $J = 9.20$ Hz, Ar), 7.91 (t, 1H, $J = 1.60$ Hz, Ar), 7.93 (d, 1H, $J = 2.40$ Hz, Ar), 8.30 (t, 1H, $J = 1.60$ Hz, Ar), 10.03 (s, 1H, NHN), 10.63 (s, 1H, NHAr), 14.50 (s, 1H, SH). Anal. Calcd for $\text{C}_{17}\text{H}_{15}\text{N}_5\text{OS}_2$ (MW 369.46): C, 55.26; H, 4.09; N, 18.96. Found: C, 55.34; H, 4.14; N, 18.87.

6.3.32. 3-(5-Sulfanyl-1,3,4-oxadiazol-2-yl)anilino-4H-1,2,4-triazol-4-ylaminomethane thione (42)

Yield: 78%, mp: 211–213 °C. IR: 1368 (C=S), 1645 (C=N), 2670 (SH), 3190 (NH) cm^{-1} ; ^1H NMR (δ ppm, DMSO- d_6 , 400 MHz): 7.53 (t, 1H, $J = 7.20$ Hz, Ar), 7.71 (d, 2H, $J = 6.40$ Hz, Ar), 8.21 (s, 1H, Ar), 8.73 (s, 2H, Tr), 9.98 (s, 1H, NHAr), 10.87 (s, 1H, NHTr), 14.18 (s, 1H, SH). Anal. Calcd for $\text{C}_{11}\text{H}_9\text{N}_7\text{OS}_2$ (MW 319.37): C, 41.37; H, 2.84; N, 30.70. Found: C, 41.41; H, 2.76; N, 30.77.

6.3.33. Piperidino-3-(5-sulfanyl-1,3,4-oxadiazol-2-yl) anilino-methanethione (43)

Yield: 81%, mp: 186–188 °C. IR: 1345 (C=S), 1546 (C=N), 2620 (SH), 3180 (NH) cm^{-1} ; ^1H NMR (δ ppm, DMSO- d_6 , 400 MHz): 1.68 (s, 6H, 3CH_2), 3.76 (s, 4H, $\text{N}(\text{CH}_2)_2$), 7.35–7.98 (m, 4H, Ar), 9.48 (s, 1H, NH), 14.05 (s, 1H, SH). Anal. Calcd for $\text{C}_{14}\text{H}_{16}\text{N}_4\text{OS}_2$ (MW 320.43): C, 52.48; H, 5.03; N, 17.48. Found: C, 52.55; H, 5.12; N, 17.51.

6.3.34. Hydrazino-3-(5-sulfanyl-1,3,4-oxadiazol-2-yl) anilino-methanethione (44)

Yield: 84%, mp: 186–187 °C. IR: 1345 (C=S), 1615 (C=N), 2729 (SH), 2862 (NH) cm^{-1} ; ^1H NMR (δ ppm, DMSO- d_6 , 400 MHz): 7.54–7.96 (m, 4H, Ar), 7.7 (d, 2H, $J = 6.9$ Hz, NH_2NH), 9.31 (s, 1H, NHNH_2), 9.92 (s, 1H, NHAr), 14.21 (s, 1H, SH). Anal. Calcd for $\text{C}_9\text{H}_9\text{N}_5\text{OS}_2$ (MW 267.33): C, 40.44; H, 3.39; N, 26.20. Found: C, 40.43; H, 3.43; N, 26.27.

6.3.35. Amino-3-(5-sulfanyl-1,3,4-oxadiazol-2-yl) anilino-methanethione (45)

Yield: 76%, mp: 195–196 °C. IR: 1351 (C=S), 1606 (C=N), 2726 (SH), 3450 (NH) cm^{-1} ; ^1H NMR (δ ppm, DMSO- d_6 , 400 MHz): 7.22–7.87 (m, 6H, Ar, NH_2), 9.93 (s, 2H, NH, SH). Anal. Calcd for $\text{C}_9\text{H}_8\text{N}_4\text{OS}_2$ (MW 252.32): C, 42.84; H, 3.20; N, 22.20. Found: C, 42.88; H, 3.24; N, 22.16.

6.3.36. N-(3-(5-Mercapto-1,3,4-oxadiazol-2-yl)phenyl)-2,2-dimethylhydrazinecarbothio amide (46)

Yield: 82%, mp: 197–198 °C. IR: 1335 (C=S), 1547 (C=N), 2590 (SH), 3135 (NH) cm^{-1} ; ^1H NMR (δ ppm, DMSO- d_6 , 400 MHz): 3.35 (s, 6H, 2Me), 7.55–7.76 (m, 4H, Ar), 8.19 (s, 1H, NHN), 9.88 (s, 1H, NHAr), 14.27 (s, 1H, SH). Anal. Calcd for $\text{C}_{11}\text{H}_{12}\text{N}_4\text{OS}_2$ (MW 295.38): C, 47.12; H, 4.31; N, 19.98. Found: C, 47.18; H, 4.34; N, 19.87.

6.3.37. 3-(5-Sulfanyl-1,3,4-oxadiazol-2-yl)anilino-4-toluidinomethanethione (47)

Yield: 81%, mp: 168–170 °C. IR: 1297 (C=S), 1634 (C=N), 2670 (SH), 3070 (NH) cm^{-1} ; ^1H NMR (δ ppm, DMSO- d_6 , 400 MHz): 2.32 (s, 3H, Me), 7.19–7.57 (m, 4H, $\text{MeC}_6\text{H}_4\text{NH}$), 7.76–8.01 (m, 4H, Ar), 9.76 (s, 1H, NHp-tolyl), 9.84 (s, 1H, NHAr), 14.32 (s, 1H, SH). Anal. Calcd for $\text{C}_{16}\text{H}_{14}\text{N}_4\text{OS}_2$ (MW 342.44): C, 56.12; H, 4.12; N, 16.36. Found: C, 56.20; H, 4.21; N, 16.43.

6.3.38. 1-(4-Fluorophenyl)-2-(5-3-[2-hydroxyethylamino(thioxo)methylamino]phenyl-1,3,4-oxadiazol-2-ylsulfanyl)-1-ethanone (56)

Yield: 75%, mp: 145–146 °C. IR: 1381 (C=S), 1640 (C=N), 1676 (C=O), 3480 (OH) cm^{-1} ; ^1H NMR (δ ppm, DMSO- d_6 , 400 MHz): 3.61–3.77 (m, 4H, $(\text{CH}_2)_2\text{NH}$), 4.68 (s, 1H, OH), 5.19 (s, 2H, SCH_2), 7.35–8.29 (m, 9H, Ar, NHCH_2), 11.31 (s, 1H, NHAr). Anal. Calcd for $\text{C}_{19}\text{H}_{17}\text{FN}_4\text{O}_3\text{S}_2$ (MW 432.49): C, 52.76; H, 3.96; N, 12.95. Found: C, 52.82; H, 3.94; N, 12.89.

6.3.39. 2-5-[3-Dimethylamino(thioxo)methylaminophenyl]-1,3,4-oxadiazol-2-ylsulfanyl-1-(2-naphthyl)-1-ethanone (57)

Yield: 87%, mp: 176–178 °C. IR: 1365 (C=S), 1615 (C=N), 1685 (C=O), 3189 (NH) cm^{-1} ; ^1H NMR (δ ppm, DMSO- d_6 , 400 MHz): 3.40 (s, 6H, 2Me), 5.00 (s, 2H, CH_2), 7.36–8.25 (m, 11H, Ar), 8.62 (s, 1H, NH). Anal. Calcd for $\text{C}_{23}\text{H}_{20}\text{N}_4\text{O}_2\text{S}_2$ (MW 448.56): C, 61.58; H, 4.49; N, 12.49. Found: C, 61.65; H, 4.44; N, 12.52.

6.3.40. 2-(5-3-[2-Hydroxyethylamino(thioxo)methylamino]phenyl-1,3,4-oxadiazol-2-ylsulfanyl)-1-(2-naphthyl)-1-ethanone (58)

Yield: 77%, mp: 153–154 °C. IR: 1472 (C=S), 1534 (C=N), 1675 (C=O), 3470 (OH) cm^{-1} ; ^1H NMR (δ ppm, DMSO- d_6 , 400 MHz): 3.53–3.59 (m, 4H, $(\text{CH}_2)_2\text{NH}$), 4.87 (s, 1H, OH), 5.31 (s, 2H, SCH_2), 7.37–8.22 (m, 12H, Ar, NHCH_2), 9.82 (s, 1H, NHAr). Anal. Calcd for $\text{C}_{23}\text{H}_{20}\text{N}_4\text{O}_3\text{S}_2$ (MW 464.56): C, 59.46; H, 4.34; N, 12.06. Found: C, 59.51; H, 4.27; N, 12.12.

6.3.41. 1-(2,4-Dichlorophenyl)-2-(5-3-[2-hydroxyethylamino(thioxo)methylamino]-phenyl-1,3,4-oxadiazol-2-ylsulfanyl)-1-ethanone (59)

Yield: 78%, mp: 83–85 °C. IR: 1457 (C=S), 1535 (C=N), 1654 (C=O), 3560 (OH) cm^{-1} ; ^1H NMR (δ ppm, DMSO- d_6 , 400 MHz): 3.53–3.59 (m, 4H, $(\text{CH}_2)_2\text{NH}$), 4.86 (s, 1H, OH), 5.00 (s, 2H, SCH_2), 7.38–8.21 (m, 8H, Ar, NHCH_2), 9.82 (s, 1H, NHAr). Anal. Calcd for $\text{C}_{19}\text{H}_{16}\text{Cl}_2\text{N}_4\text{O}_3\text{S}_2$ (MW 483.39): C, 47.21; H, 3.34; N, 11.59. Found: C, 47.24; H, 3.37; N, 11.62.

6.3.42. 2-5-[3-Amino(thioxo)methylaminophenyl]-1,3,4-oxadiazol-2-ylsulfanyl-1-(2,4-dichlorophenyl)-1-ethanone (60)

Yield: 64%, mp: 200–202 °C. IR: 1475 (C=S), 1618 (C=N), 1662 (C=O), 3450 (NH_2) cm^{-1} ; ^1H NMR (δ ppm, DMSO- d_6 , 400 MHz): 5.01 (s, 2H, CH_2), 7.36–8.15 (m, 9H, Ar, NH_2), 9.93 (s, 1H, NH). Anal. Calcd for $\text{C}_{17}\text{H}_{12}\text{Cl}_2\text{N}_4\text{O}_2\text{S}_2$ (MW 439.34): C, 46.47; H, 2.75; N, 12.75. Found: C, 46.49; H, 2.79; N, 12.72.

6.3.43. 2-5-[3-Amino(thioxo)methylaminophenyl]-1,3,4-oxadiazol-2-ylsulfanyl-1-(4-chlorophenyl)-1-ethanone (61)

Yield: 81%, mp: 193–194 °C. IR: 1460 (C=S), 1579 (C=N), 1665 (C=O), 3445 (NH₂) cm⁻¹; ¹H NMR (δ ppm, DMSO-*d*₆, 400 MHz): 5.15 (s, 2H, CH₂), 7.35–7.72 (m, 6H, Ar, NH₂), 8.00–8.13 (m, 4H, Ar), 9.92 (s, 1H, NH). Anal. Calcd for C₁₇H₁₃ClN₄O₂S₂ (MW 404.89): C, 50.43; H, 3.24; N, 13.84. Found: C, 50.47; H, 3.27; N, 13.89.

6.3.44. 2-5-[3-Amino(thioxo)methylaminophenyl]-1,3,4-oxadiazol-2-ylsulfanyl-1-phenyl-1-ethanone (62)

Yield: 74%, mp: 180–182 °C. IR: 1476 (C=S), 1665 (C=N), 1657 (C=O), 3350 (NH₂) cm⁻¹; ¹H NMR (δ ppm, DMSO-*d*₆, 400 MHz): 5.18 (s, 2H, CH₂), 7.36–8.14 (m, 11H, Ar, NH₂), 9.92 (s, 1H, NH). Anal. Calcd for C₁₇H₁₄N₄O₂S₂ (MW 370.45): C, 55.12; H, 3.81; N, 15.12. Found: C, 55.16; H, 3.88; N, 15.16.

6.3.45. 2-5-[3-Amino(thioxo)methylaminophenyl]-1,3,4-oxadiazol-2-ylsulfanyl-1-(4-bromophenyl)-1-ethanone (63)

Yield: 89%, mp: 187–188 °C. IR: 1467 (C=S), 1598 (C=N), 1645 (C=O), 3045 (NH₂) cm⁻¹; ¹H NMR (δ ppm, DMSO-*d*₆, 400 MHz): 5.16 (s, 2H, CH₂), 7.36–8.13 (m, 10H, Ar, NH₂), 9.94 (s, 1H, NH). Anal. Calcd for C₁₇H₁₃BrN₄O₂S₂ (MW 449.34): C, 45.44; H, 2.92; N, 12.47. Found: C, 45.48; H, 2.96; N, 12.51.

6.3.46. 2-5-[3-Dimethylamino(thioxo)methylaminophenyl]-1,3,4-oxadiazol-2-ylsulfanyl-1-phenyl-1-ethanone (64)

Yield: 80%, mp: 166–168 °C. IR: 1377 (C=S), 1656 (C=N), 1445 (C=O), 3268 (NH) cm⁻¹; ¹H NMR (δ ppm, DMSO-*d*₆, 400 MHz): 3.40 (s, 6H, 2Me), 5.01 (s, 2H, CH₂), 7.25–8.00 (m, 9H, Ar), 8.61 (s, 1H, NH). Anal. Calcd for C₁₉H₁₈N₄O₂S₂ (MW 398.50): C, 57.26; H, 4.55; N, 14.06. Found: C, 57.28; H, 4.52; N, 14.11.

6.3.47. Amino-3-(5-phenethylsulfanyl-1,3,4-oxadiazol-2-yl)anilinomethanethione (65)

Yield: 78%, mp: 127–128 °C. IR: 1465 (C=S), 1765 (C=N), 2738 (SCH₂), 3430 (NH₂) cm⁻¹; ¹H NMR (δ ppm, DMSO-*d*₆, 400 MHz): 3.08 (t, 2H, *J* = 7.46 Hz, CH₂S), 3.57 (t, 2H, *J* = 7.46 Hz, CH₂Ar), 7.25–8.17 (m, 11H, Ar, NH₂), 9.95 (s, 1H, NH). Anal. Calcd for C₁₇H₁₆N₄OS₂ (MW 356.47): C, 57.28; H, 4.52; N, 15.72. Found: C, 57.32; H, 4.54; N, 15.76.

6.3.48. 1-(4-Bromophenyl)-2-(5-3-[2-hydroxyethylamino(thioxo)methylamino]phenyl-1,3,4-oxadiazol-2-ylsulfanyl)-1-ethanone (66)

Yield: 84%, mp: 162–164 °C. IR: 1367 (C=S), 1541 (C=N), 1644 (C=O), 3290 (OH) cm⁻¹; ¹H NMR (δ ppm, DMSO-*d*₆, 400 MHz): 3.52–3.58 (m, 4H, (CH₂)₂NH), 4.89 (s, 1H, OH), 5.16 (s, 2H, SCH₂), 7.56–8.19 (m, 9H, Ar, NH CH₂), 9.84 (s, 1H, NHAr). Anal. Calcd for C₁₉H₁₇BrN₄O₃S₂ (MW 493.40): C, 46.25; H, 3.47; N, 11.36. Found: C, 46.27; H, 3.51; N, 11.42.

6.3.49. 1-(4-Chlorophenyl)-2-(5-3-[2-dimethylamino(thioxo)methylaminophenyl]-1,3,4-oxadiazol-2-ylsulfanyl)-1-ethanone (67)

Yield: 92%, mp: 158–160 °C. IR: 1384 (C=S), 1615 (C=N), 1385 (C=O), 3170 (NH) cm⁻¹; ¹H NMR (δ ppm, DMSO-*d*₆, 400 MHz): 3.41 (s, 6H, 2Me), 5.00 (s, 2H, SCH₂), 7.38–8.02 (m, 8H, Ar), 8.60 (s, 1H, NH). Anal. Calcd for C₁₉H₁₇ClN₄O₂S₂ (MW 432.95): C, 52.71; H, 3.96; N, 12.94. Found: C, 52.75; H, 3.92; N, 12.97.

6.3.50. 2-5-[3-Amino(thioxo)methylaminophenyl]-1,3,4-oxadiazol-2-ylsulfanyl-1-(4-fluorophenyl)-1-ethanone (68)

Yield: 87%, mp: 190–192 °C. IR: 1471 (C=S), 1610 (C=N), 1648 (C=O), 3303 (NH₂) cm⁻¹; ¹H NMR (δ ppm, DMSO-*d*₆, 400 MHz): 5.17 (s, 2H, CH₂), 7.31–8.25 (m, 10H, Ar, NH₂), 9.94 (s, 1H, NH).

Anal. Calcd for C₁₇H₁₃FN₄O₂S₂ (MW 388.44): C, 52.56; H, 3.37; N, 14.42. Found: C, 52.59; H, 3.38; N, 14.48.

6.3.51. 2-(5-3-[2-Hydroxyethylamino(thioxo)methylamino]phenyl-1,3,4-oxadiazol-2-ylsulfanyl)-1-phenyl-1-ethanone (69)

Yield: 89%, mp: 150–152 °C. IR: 1455 (C=S), 1490 (C=N), 1675 (C=O), 3256 (OH) cm⁻¹; ¹H NMR (δ ppm, DMSO-*d*₆, 400 MHz): 3.53–3.56 (m, 4H, (CH₂)₂NH), 4.90 (s, 1H, OH), 5.18 (s, 2H, SCH₂), 7.47–8.19 (m, 10H, Ar, NHCH₂), 9.84 (s, 1H, NHAr). Anal. Calcd for C₁₉H₁₈N₄O₃S₂ (MW 414.50): C, 55.05; H, 4.38; N, 13.52. Found: C, 55.12; H, 4.42; N, 13.55.

6.3.52. 2-5-[3-Dimethylamino(thioxo)methylaminophenyl]-1,3,4-oxadiazol-2-ylsulfanyl-1-(4-methylphenyl)-1-ethanone (70)

Yield: 90%, mp: 173–175 °C. IR: 1384 (C=S), 1645 (C=N), 1467 (C=O), 3240 (NH) cm⁻¹; ¹H NMR (δ ppm, DMSO-*d*₆, 400 MHz): 2.32 (s, 3H, MeAr), 3.41 (s, 6H, Me₂N), 5.00 (s, 2H, SCH₂), 7.41–8.15 (m, 8H, Ar), 8.63 (s, 1H, NH). Anal. Calcd for C₂₀H₂₀N₄O₂S₂ (MW 412.53): C, 58.23; H, 4.89; N, 13.58. Found: C, 58.26; H, 4.93; N, 13.54.

6.3.53. 2-5-[3-Amino(thioxo)methylaminophenyl]-1,3,4-oxadiazol-2-ylsulfanyl-1-(2-naphthyl)-1-ethanone (71)

Yield: 82%, mp: 193–194 °C. IR: 1400 (C=S), 1645 (C=N), 1565 (C=O), 3070 (NH₂) cm⁻¹; ¹H NMR (δ ppm, DMSO-*d*₆, 400 MHz): 5.31 (s, 2H, CH₂), 7.36–8.22 (m, 13H, Ar, NH₂), 9.92 (s, 1H, NH). Anal. Calcd for C₂₁H₁₆N₄O₂S₂ (MW 420.51): C, 59.98; H, 3.84; N, 13.32. Found: C, 59.93; H, 3.86; N, 13.38.

6.3.54. 6.3.54.2-Hydroxyethylamino-3-(5-phenethylsulfanyl-1,3,4-oxadiazol-2-yl)anilinomethane thione (72)

Yield: 85%, mp: 142–144 °C. IR: 1465 (C=S), 1590 (C=N), 2547 (SCH₂), 3270 (OH) cm⁻¹; ¹H NMR (δ ppm, DMSO-*d*₆, 400 MHz): 3.01–3.18 (m, 4H, (CH₂)₂Ar), 3.47–3.65 (m, 5H, HO(CH₂)₂), 7.25–7.76 (m, 10H, Ar, NHCH₂), 8.25 (s, 1H, NHAr). Anal. Calcd for C₁₉H₂₀N₄O₂S₂ (MW 400.52): C, 56.98; H, 5.03; N, 13.99. Found: C, 56.92; H, 5.11; N, 13.92.

6.3.55. Amino-3-(5-methylsulfanyl-1,3,4-oxadiazol-2-yl)anilinomethanethione (73)

Yield: 80%, mp: 221 °C. IR: 1240 (SCH₃), 1348 (C=S), 1615 (C=N), 3490 (NH₂) cm⁻¹; ¹H NMR (δ ppm, DMSO-*d*₆, 400 MHz): 2.75 (s, 3H, Me), 7.33–7.98 (m, 6H, Ar, NH₂), 9.93 (s, 1H, NH). Anal. Calcd for C₁₀H₁₀N₄OS₂ (MW 266.34): C, 45.09; H, 3.78; N, 21.04. Found: C, 45.13; H, 3.68; N, 21.12.

6.3.56. 2-Hydroxyethylamino-3-(5-methylsulfanyl-1,3,4-oxadiazol-2-yl)anilinomethane thione (74)

Yield: 78%, mp: 150–153 °C. IR: 1356 (SCH₃), 1376 (C=S), 1645 (C=N), 3520 (OH) cm⁻¹; ¹H NMR (δ ppm, DMSO-*d*₆, 400 MHz): 2.65 (s, 3H, Me), 3.61 (s, 4H, (CH₂)₂NH), 4.88 (s, 1H, OH), 7.45–7.56 (m, 5H, Ar, NHCH₂), 9.90 (s, 1H, NHAr). Anal. Calcd for C₁₂H₁₄N₄O₂S₂ (MW 310.40): C, 46.43; H, 4.55; N, 18.05. Found: C, 46.55; H, 4.59; N, 18.12.

6.3.57. 3-(5-Methylsulfanyl-1,3,4-oxadiazol-2-yl)anilino-4H-1,2,4-triazol-4-ylamino methanethione (75)

Yield: 69%, mp: 182–184 °C. IR: 1210 (SCH₃), 1375 (C=S), 1645 (C=N), 3240 (NH) cm⁻¹; ¹H NMR (δ ppm, DMSO-*d*₆, 400 MHz): 2.78 (s, 3H, Me), 7.55 (t, 1H, *J* = 7.60 Hz, Ar), 7.76 (d, 2H, *J* = 6.80 Hz, Ar), 8.15 (s, 1H, Ar), 8.68 (s, 2H, Tr), 10.63 (s, 1H, NHAr), 11.08 (s, 1H, NHTr). Anal. Calcd for C₁₂H₁₁N₇OS₂ (MW 333.39): C, 43.23; H, 3.33; N, 29.41. Found: C, 43.27; H, 3.41; N, 29.47.

6.3.58. Hydrazino-3-(5-methylsulfanyl-1,3,4-oxadiazol-2-yl)anilinomethanethione (76)

Yield: 72%, mp: 141–143 °C. IR: 1234 (SCH₃), 1475 (C=S), 1625 (C=N), 3390 (NH₂) cm⁻¹; ¹H NMR (δ ppm, DMSO-*d*₆, 400 MHz): 2.76 (s, 3H, Me), 7.56–7.89 (m, 4H, Ar), 7.89 (d, 2H, *J* = 6.8 Hz, NH₂NH), 9.36 (s, 1H, NHNH₂), 10.15 (s, 1H, NHAr). Anal. Calcd for C₁₀H₁₁N₅OS₂ (MW 281.36): C, 42.69; H, 3.94; N, 24.89. Found: C, 42.66; H, 3.91; N, 24.77.

6.3.59. 3-(5-Methylsulfanyl-1,3,4-oxadiazol-2-yl)anilino-4-toluidinomethanethione (77)

Yield: 74%, mp: 173–175 °C. IR: 1167 (SCH₃), 1365 (C=S), 1645 (C=N), 3090 (NH) cm⁻¹; ¹H NMR (δ ppm, DMSO-*d*₆, 400 MHz): 2.35 (s, 3H, MeAr), 2.78 (s, 3H, SMe), 7.25–7.68 (m, 4H, MeC₆H₄NH), 7.81–8.12 (m, 4H, Ar), 9.84 (s, 1H, NHp-tolyl), 9.96 (s, 1H, NHAr). Anal. Calcd for C₁₇H₁₆N₄O₂S₂ (MW 356.47): C, 57.28; H, 4.52; N, 15.72. Found: C, 57.31; H, 4.58; N, 15.79.

6.3.60. 3-(5-Methylsulfanyl-1,3,4-oxadiazol-2-yl)anilino-morpholinomethanethione (78)

Yield: 79%, mp: 134–136 °C. IR: 1225 (SCH₃), 1346 (C=S), 1638 (C=N), 3192 (NH) cm⁻¹; ¹H NMR (δ ppm, DMSO-*d*₆, 400 MHz): 2.75 (s, 3H, Me), 3.67 (t, 4H, *J* = 4.8 Hz, 2OCH₂), 3.95 (t, 4H, *J* = 4.8 Hz, N(CH₂)₂), 7.46–7.81 (m, 4H, Ar), 9.54 (s, 1H, NH). Anal. Calcd for C₁₄H₁₆N₄O₂S₂ (MW 336.43): C, 49.98; H, 4.79; N, 16.65. Found: C, 49.86; H, 4.75; N, 16.77.

6.3.61. 3-(5-Methylsulfanyl-1,3,4-oxadiazol-2-yl)anilino-methanethione (79)

Yield: 65%, mp: 161–162 °C. IR: 1335 (C=S), 1545 (C=N), 2600 (SH), 3197 (N(CH₃)₂) cm⁻¹; ¹H NMR (δ ppm, DMSO-*d*₆, 400 MHz): 2.12 (s, 6H, 2Me), 2.58 (s, 3H, SMe), 7.38–7.57 (m, 4H, Ar), 9.25 (s, 1H, NHN), 9.90 (s, 1H, NHAr). Anal. Calcd for C₁₂H₁₄N₄O₂S₂ (MW 294.40): C, 48.96; H, 4.79; N, 19.03. Found: C, 48.89; H, 4.82; N, 19.12.

6.3.62. 1-(2,4-Dichlorophenyl)-2,5-[3-dimethylamino(thioxo)methylaminophenyl]-1,3,4-oxadiazol-2-ylsulfanyl-1-ethanone (80)

Yield: 80%, mp: 79–81 °C. IR: 1315 (C=S), 1618 (C=N), 1647 (C=O), 3098 (NH) cm⁻¹; ¹H NMR (δ ppm, DMSO-*d*₆, 400 MHz): 3.41 (s, 6H, 2Me), 5.00 (s, 2H, CH₂), 7.25–8.01 (m, 7H, Ar), 8.60 (s, 1H, NH). Anal. Calcd for C₁₉H₁₆Cl₂N₄O₂ (MW 467.39): C, 48.82; H, 3.45; N, 11.99. Found: C, 48.91; H, 3.48; N, 12.04.

6.3.63. Amino-3-(5-benzylsulfanyl-1,3,4-oxadiazol-2-yl)anilinomethanethione (81)

Yield: 86%, mp: 177–179 °C. IR: 1463 (C=S), 1656 (C=N), 2727 (SCH₂), 3345 (NH₂) cm⁻¹; ¹H NMR (δ ppm, DMSO-*d*₆, 400 MHz): 4.57 (s, 2H, CH₂), 6.95–8.39 (m, 11H, Ar, NH₂), 9.93 (s, 1H, NH). Anal. Calcd for C₁₆H₁₄N₄O₂S (MW 342.44): C, 56.12; H, 4.12; N, 16.36. Found: C, 56.16; H, 4.21; N, 16.41.

6.3.64. 2-5-[3-Methylamino(thioxo)methylaminophenyl]-1,3,4-oxadiazol-2-ylsulfanyl-1-(2-naphthyl)-1-ethanone (82)

Yield: 80%, mp: 201–203 °C. IR: 1377 (C=S), 1615 (C=N), 1687 (C=O), 3190 (NH) cm⁻¹; ¹H NMR (δ ppm, DMSO-*d*₆, 400 MHz): 2.33 (d, 3H, *J* = 3.98 Hz, Me), 5.02 (s, 2H, SCH₂), 7.68–8.02 (m, 11H, Ar), 8.15 (s, 1H, NHMe), 9.76 (s, 1H, NHAr). Anal. Calcd for C₂₂H₁₈N₄O₂S₂ (MW 434.53): C, 60.81; H, 4.18; N, 12.89. Found: C, 60.93; H, 4.22; N, 12.94.

7. In vitro evaluation of the antituberculosis activity

Primary screening was conducted at 6.25 µg/mL against *M. tuberculosis* H₃₇Rv (ATCC 27294) in BACTEC 12B medium using a

broth microdilution assay, the Microplate Alamar Blue Assay (MABA) according to the reported method.²⁶

Acknowledgments

The authors gratefully acknowledge funding through a grant from the Moldavian-US Bilateral Grants Program of the US Civilian Research and Development Foundation (Grant MC2-3007). We also acknowledge the Tuberculosis Antimicrobial Acquisition and Coordinating Facility provided through the US National Institutes of Health (Contract N01-AI-95364) for providing data on the antitubercular activity.

Supplementary data

Supplementary data associated with this article can be found, in the online version, at [doi:10.1016/j.bmc.2011.09.038](https://doi.org/10.1016/j.bmc.2011.09.038). These data include MOL files and InChIKeys of the most important compounds described in this article.

References and notes

- Janin, Y. L. *Bioorg. Med. Chem.* **2007**, *15*, 2479.
- Murray, Christopher, J. L.; Lopez, Alan, D. *The Global Burden of Disease: A Comprehensive Assessment of Mortality and Disability from Diseases, Injuries and Risk Factors in 1990 and Projected to 2020: Summary*; WHO: Switzerland, 1996.
- Narain, J. P. In *Tuberculosis-Epidemiology and Control*; World Health Organization: New Delhi, India, 2002; Vol. 248, pp 15–18.
- Fattorini, L.; Iona, E.; Ricci, M. L.; Thoresen, O. F.; Orrù, G.; Oggioni, M. R.; Tortoli, E.; Piersimoni, C.; Chiaradonna, P.; Tronci, M.; Pozzi, G.; Orefici, G. *Microb. Drug Resist.* **1999**, *5*, 265.
- Van Rie, A.; Warren, R. M.; Beyers, N.; Gie, R. P.; Classen, C. N.; Richardson, M.; Sampson, S. L.; Victor, T. C.; Van Helden, P. D. *J. Infect. Dis.* **1999**, *180*, 1608.
- Enwere, G. C.; Ota, M. O.; Obaro, S. K. *Ann. Trop. Med. Parasitol.* **1999**, *93*, 669.
- Smith, K.; Bender, J.; Osterholm, M.; Nachamkin, I.; Blaser, M. *Campylobacter*; American Society for Microbiology: Washington, DC, 2000. pp 483–495.
- World Health Organization. In *Antituberculosis Drug Resistance in the World*; The WHO/IUATLD Global Project on Antituberculosis Drug Resistance Surveillance. Switzerland, 1997.
- Ballell, L.; Field, R. A.; Duncan, K.; Young, R. J. *Antimicrob. Agents Chemother.* **2005**, *49*, 2153.
- Sutherland, H. S.; Blaser, A.; Kmentova, I.; Franzblau, S. G.; Wan, B.; Wang, Y.; Ma, Z.; Palmer, B. D.; Denny, W. A.; Thompson, A. M. *J. Med. Chem.* **2010**, *53*, 855.
- Navarrete-Vázquez, G.; Molina-Salinas, G. M.; Duarte-Fajardo, Z. V.; Vargas-Villalreal, J.; Estrada-Soto, S.; González-Salazar, F.; Hernández-Núñez, E.; Said-Fernández, S. *Bioorg. Med. Chem.* **2007**, *15*, 5502.
- Khan, R. H.; Rastogi, R. C. *J. Agric. Food Chem.* **1990**, *38*, 1068.
- Narayana, B.; Raj, K. K. V.; Ashalatha, B. V.; Kumari, N. S. *Arch. Pharm. Chem. Life Sci.* **2005**, *338*, 373.
- Schelenz, T.; Klunker, J.; Bernhardt, T.; Schafer, W.; Dost, J. *Quant. Struct.-Act. Relat.* **2001**, *20*, 291.
- Macaev, F.; Rusu, G.; Pogrebnoi, S.; Gudima, A.; Stingaci, E.; Vlad, L.; Shvets, N.; Kandemirli, F.; Dimoglo, A.; Reynolds, R. *Bioorg. Med. Chem.* **2005**, *13*, 4842.
- Klimesova, V.; Zahajska, L.; Waissner, K.; Kaustova, J.; Möllmann, U. *Farmaco* **2004**, *59*, 279.
- Mir, I.; Siddiqui, M. T. *Tetrahedron* **1970**, *26*, 5235.
- Ulusoy, N.; Gürsoy, A.; Ötük, G. *Farmaco* **2001**, *56*, 947.
- Kaplançıklı, S. A.; Turan-Zitouni, G.; Chevallet, P. *J. Enzyme Inhib. Med. Chem.* **2005**, *20*, 179.
- Dimoglo, A.; Kovalishyn, V.; Shvets, N.; Ahsen, V. *Mini-Rev. Med. Chem.* **2005**, *5*, 879.
- Dimoglo, A. S.; Vlad, P. F.; Shvets, N. M.; Coltsa, M. N. *N. J. Chem.* **2001**, *25*, 283.
- Dimoglo, A. S.; Shvets, N. M.; Tetko, I. V.; Livingstone, D. J. *Quant. Struct.-Act. Relat.* **2001**, *20*, 31.
- Dimoglo, A.; Sim, E.; Shvets, N.; Ahsen, V. *Mini-Rev. Med. Chem.* **2003**, *3*, 293.
- Sim, E.; Dimoglo, A.; Shvets, N.; Ahsen, V. *Curr. Med. Chem.* **2002**, *9*, 1537.
- Oruç, E.; Rollas, S.; Kandemirli, F.; Shvets, N.; Dimoglo, A. *J. Med. Chem.* **2004**, *47*, 6760.
- Koçyiğit-Kaymakçioğlu, B.; Oruç, E.; Unsalan, S.; Kandemirli, F.; Shvets, N.; Rollas, S.; Dimoglo, A. *Eur. J. Med. Chem.* **2006**, *41*, 1253.
- Rusu, G. G.; Gutu, E. E.; Barba, N. A. *Russ. J. Org. Chem.* **1995**, *31*, 1721.
- Collins, L.; Franzblau, S. G. *Antimicrob. Agents Chemother.* **1997**, *41*, 1004.
- Wermuth, C. G. *The Practice of Medicinal Chemistry*; Academic Press: San Diego, 1996. pp 81–99.
- Cohen, N. C. *Compendium on Molecular Modelling in Drug Design*; Academic Press: San Diego, 1996. p 361.
- PDB ID:1C10. Shi, W.; Ostrov, D.A.; Gerchman, S.E.; Graziano, V.; Kycia, H.; Studier, B.; Almo, S.C.; Burley, S.K. New York Structural Genomics Research Consortium (NYSGRXRC).

32. Biswal, B. K.; Cherney, M. M.; Wang, M.; Garen, C.; James, M. N. *Acta Crystallogr.* **2005**, D61, 1492.
33. Canaan, S.; Sulzenbacher, G.; Roig-Zamboni, V.; Scappuccini-Calvo, L.; Frassinetti, F.; Maurin, D.; Cambillau, C.; Bourne, Y. *FEBS Lett.* **2005**, 579, 215.
34. Molecular Operating Environment (MOE) software, release 2008.10.
35. Dewar, M. J. S.; Zoebisch, E. G.; Healy, E. F.; Stewart, J. J. P. *J. Am. Chem. Soc.* **1985**, 107, 3902.
- [36]. Frisch, M. J.; Trucks, G. W.; Schlegel, H. B.; Scuseria, G. E.; Robb, M. A.; Cheeseman, J. R.; Montgomery, J. A., Jr.; Vreven, T.; Kudin, K. N.; Burant, J. C.; Millam, J. M.; Iyengar, S. S.; Tomasi, J.; Barone, V.; Mennucci, B.; Cossi, M.; Scalmani, G.; Rega, N.; Petersson, G. A.; Nakatsuji, H.; Hada, M.; Ehara, M.; Toyota, K.; Fukuda, R.; Hasegawa, J.; Ishida, M.; Nakajima, T.; Honda, Y.; Kitao, O.; Nakai, H.; Klene, M.; Li, X.; Knox, J. E.; Hratchian, H. P.; Cross, J. B.; Adamo, C.; Jaramillo, J.; Gomperts, R.; Stratmann, R. E.; Yazyev, O.; Austin, A. J.; Cammi, R.; Pomelli, C.; Ochterski, J. W.; Ayala, P. Y.; Morokuma, K.; Voth, G. A.; Salvador, P.; Dannenberg, J. J.; Zakrzewski, V. G.; Dapprich, S.; Daniels, A. D.; Strain, M. C.; Farkas, O.; Malick, D. K.; Rabuck, A. D.; Raghavachari, K.; Foresman, J. B.; Ortiz, J. V.; Cui, Q.; Baboul, A. G.; Clifford, S.; Cioslowski, J.; Stefanov, B. B.; Liu, G.; Liashenko, A.; Piskorz, P.; Komaromi, I.; Martin, R. L.; Fox, D. J.; Keith, T.; Al-Laham, M. A.; Peng, C. Y.; Nanayakkara, A.; Challacombe, M.; Gill, P. M. W.; Johnson, B.; Chen, W.; Wong, M. W.; Gonzalez, C.; Pople, J. A. *GAUSSIAN-03*, Revision A.1, Gaussian: Pittsburgh, PA, 2003.
37. Dimoglo, A. S. *Khim. Pharm. Zhur.* **1985**, 4, 438.
38. Dimoglo, A. S. In *Book 'Coordination and Organic Biologically Active Compounds'*; Kishinev, 1986. pp 7–11.
39. Bersuker, I. B.; Dimoglo, A. S. In *Reviews in Computational Chemistry*; Lipkowitz, K. B., Boyd, D. B., Eds.; VCH: New-York, 1991. Chapter 10.
40. Shvets, N. M.; Dimoglo, A. S. *Nahrung* **1998**, 42, 364.
41. Cramer, R. D.; DePriest, S. A.; Patterson, D. E.; Hecht, P. In *3D QSAR in Drug Design: Theory Methods and Applications*; Kubinyi, H., Ed.; ESCOM: Leiden: The Netherlands, 1993; pp 443–486.
42. Tetko, I. V. *J. Chem. Inf. Comput. Sci.* **2002**, 42, 717.
43. Tetko, I. V.; Livingstone, D. J.; Luik, A. I. *J. Chem. Inf. Comput. Sci.* **1995**, 35, 826.
44. Tetko, I. V.; Kovalishyn, V. V.; Livingstone, D. J. *J. Med. Chem.* **2001**, 44, 2411.
45. Tetko, I. V.; Villa, A. E. P.; Livingstone, D. J. *J. Chem. Inf. Comput. Sci.* **1996**, 36, 794.
46. Kovalishyn, V. V.; Tetko, I. V.; Luik, A. I.; Kholodovych, V. V.; Villa, A. E. P.; Livingstone, D. J. *J. Chem. Inf. Comput. Sci.* **1998**, 38, 651.